Lagrangian approach: Stirred and mixed (but not shaken)

Hezi Gildor

Institute of Earth Sciences

The Hebrew University

Phytoplankton bloom in the Norwegian Sea, SeaWiFs

From Tel et al. 2005

Thanks to
Dan Carlson, Erick Fredj, Vered Rom-Kedar

ISRAEL SCIENCE FOUNDATION

משרד המדע, הטכנולוגיה והחלל
Ministry of Science, Technology and Space
وزارة العلوم، التكنولوجيا والفضاء

Do we need submeso and fine-scale measurements?

"The ocean has no physics, and so there is no need for observations. Oceanographers should be forced to stay at home and run models" - quote taken from Wunsch 2002 (NOT his view!).

"…. I figured that I should go to sea at least once if I was going to call myself an oceanographer. Prof. X, a well-known theoretician who was my major professor, disagreed. His initial view was that there was nothing in oceanography that couldn't be learned from behind his desk." - quote taken from Chapman 2004.

The more one is able to observe the ocean, the more the complexity and subtlety that appears.

Submesoscale processes – a gap in observations and understanding

Large scale
(1000s km, 18th century)

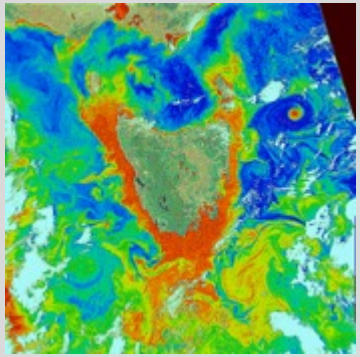

Mesoscale
(10s km, 1970s)

Submesoscale
O(1) km

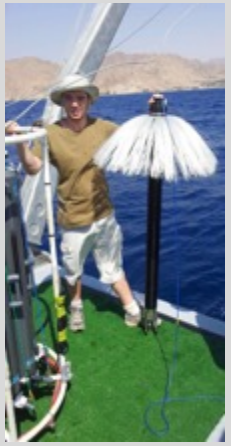

Fine-scale turbulence
(mm-cm-m)

MERCI –
Mediterranean Sea Research Center of Israel

- Founded following the recent discoveries of natural gas off the coast of Israel, managed by Haifa University.
- Seven of universities, a college and two governmental research institutes (IOLR and the Geological Survey)
- New technologies, including AUV, ROV, gliders

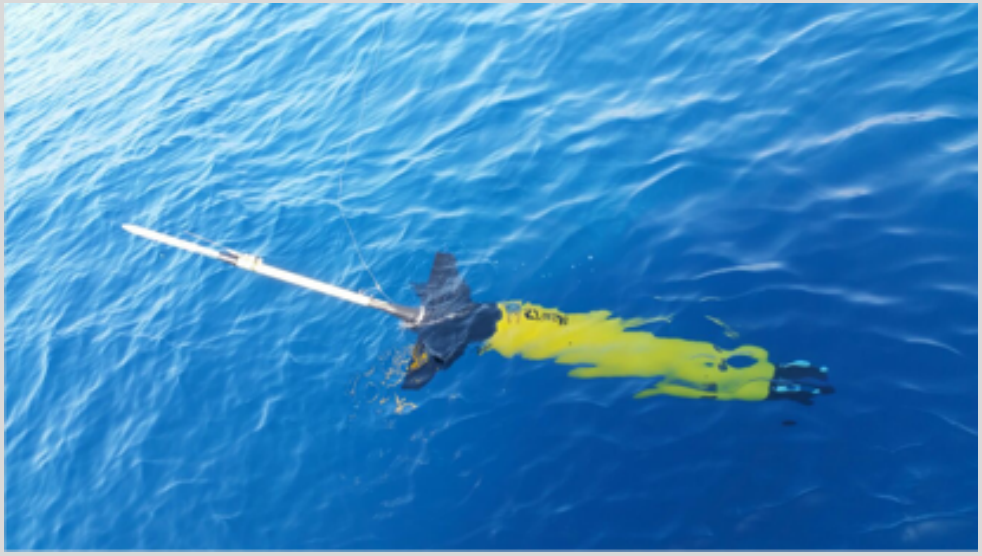

WIS, HUJI, IOLR, BIU

OGS, OC-UCY

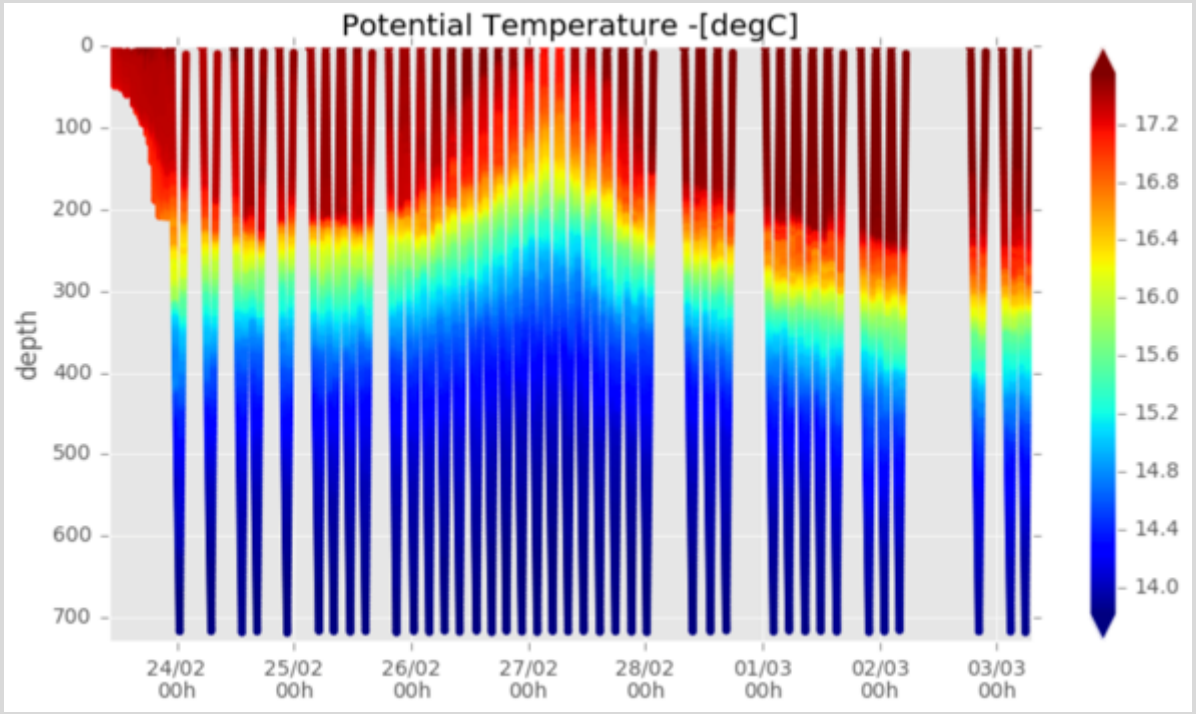

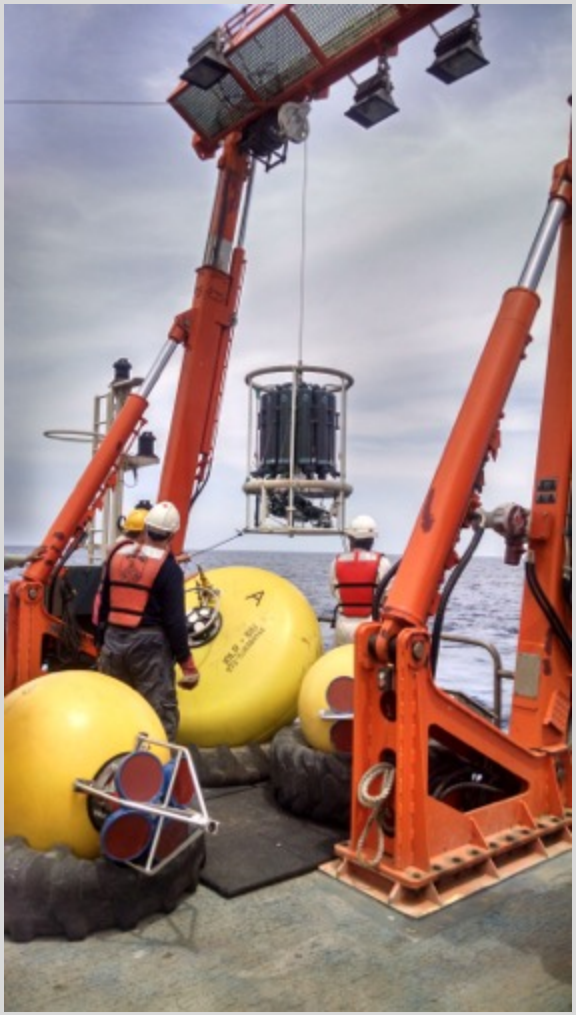

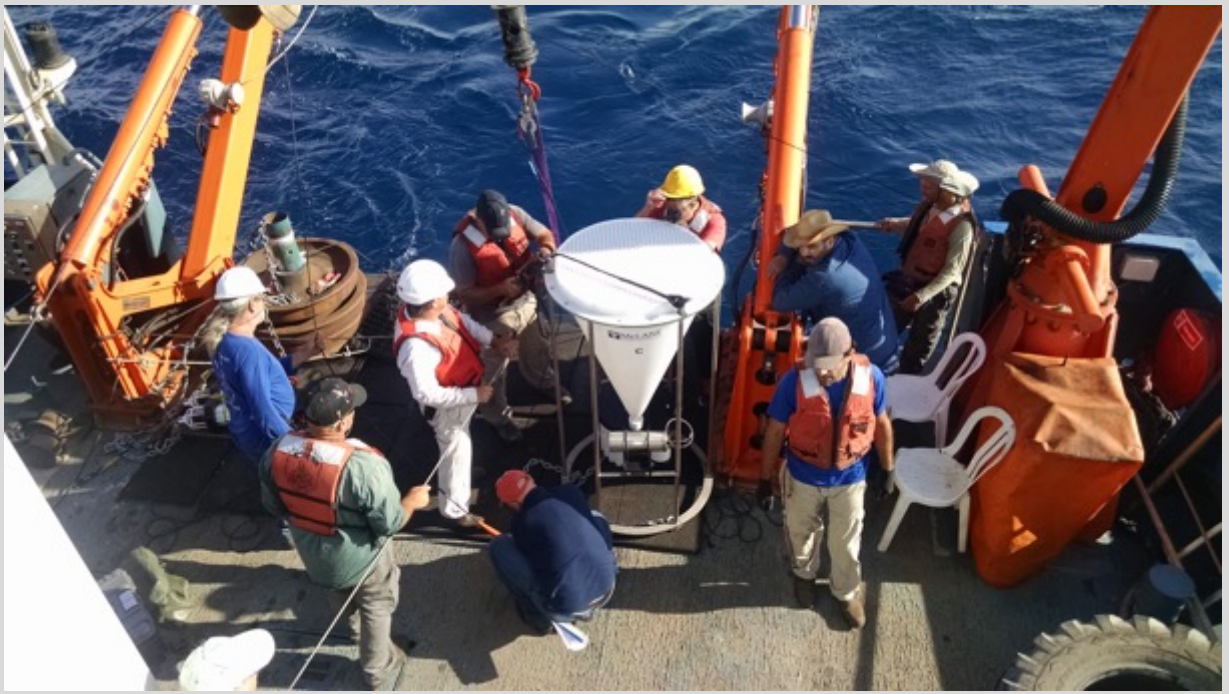

1500 m mooring: BIU, IOLR, TAU, HUJI

HF radar network

Shikmona gyre area

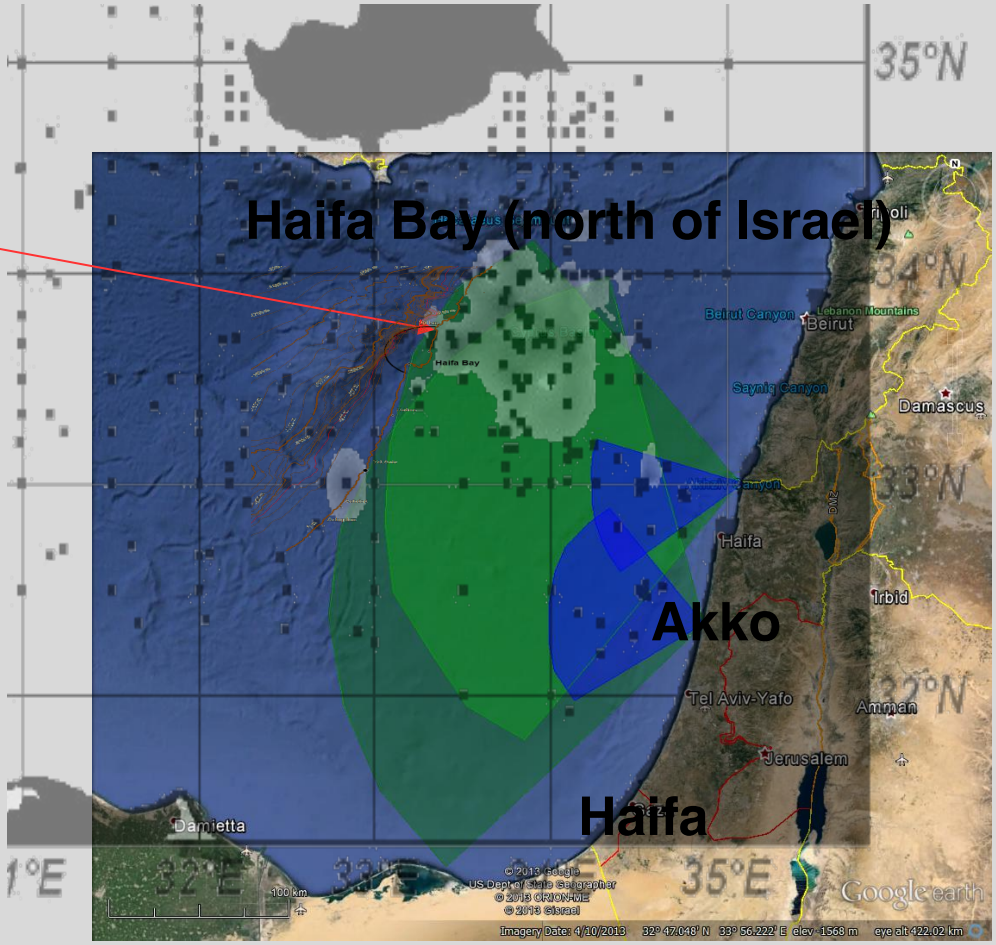

Yaron Toledo, TAU

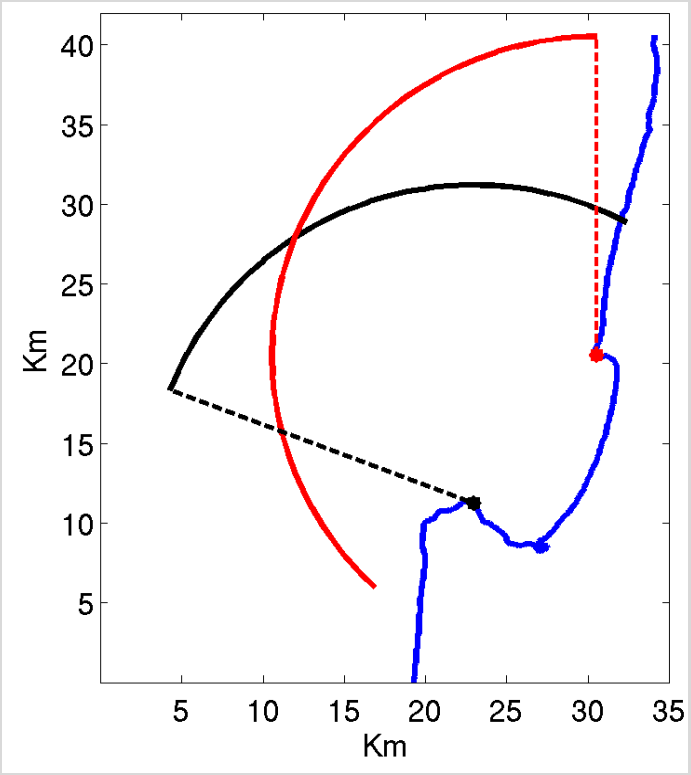

HUJI, IOLR

Numerical simulations

- MITgcm (Massachusetts Institute of Technology) ocean general circulation model
- $1/8^0$ degree horizontal and 22 vertical layers unevenly spaced (7 in the upper 150 m); bathymetry is based on ETOPO2
- Wind-stress is derived from the monthly climatology of ERA-Interim reanalysis
- B.C. and I.C. for temperature and salinity are derived from NEMO-MED reanalysis
- Mixed b.c. after 1500 yr of spin-up

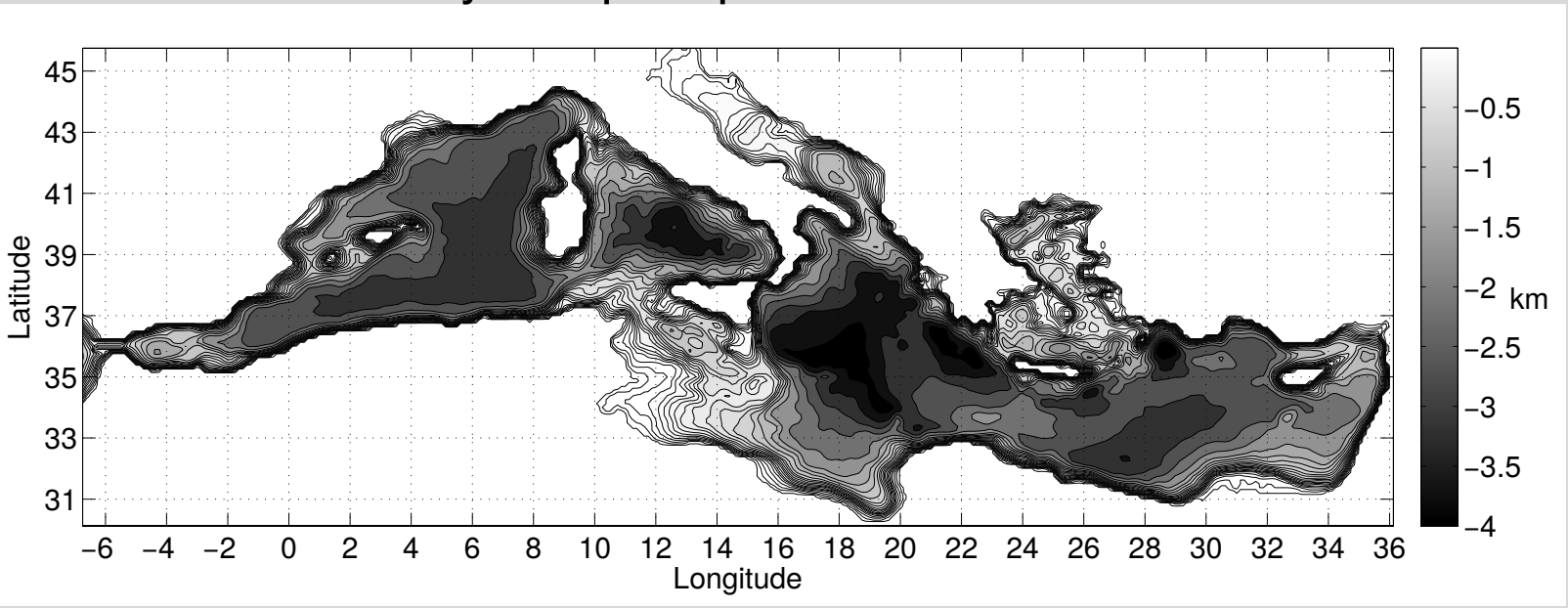

Multiple equilibria of dense water outflow

Adriatic

Aegean

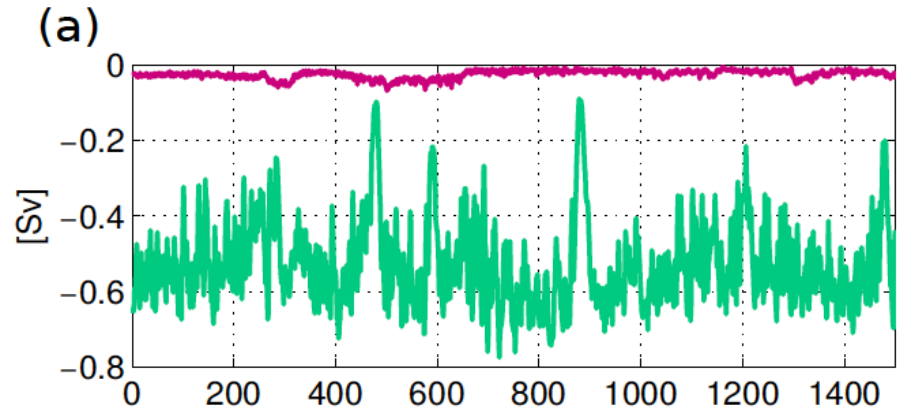

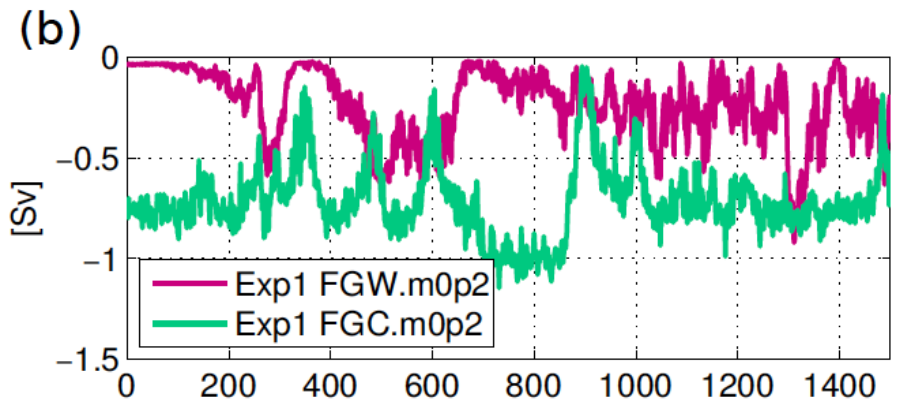

- Steady-states are stable for 1500 yr

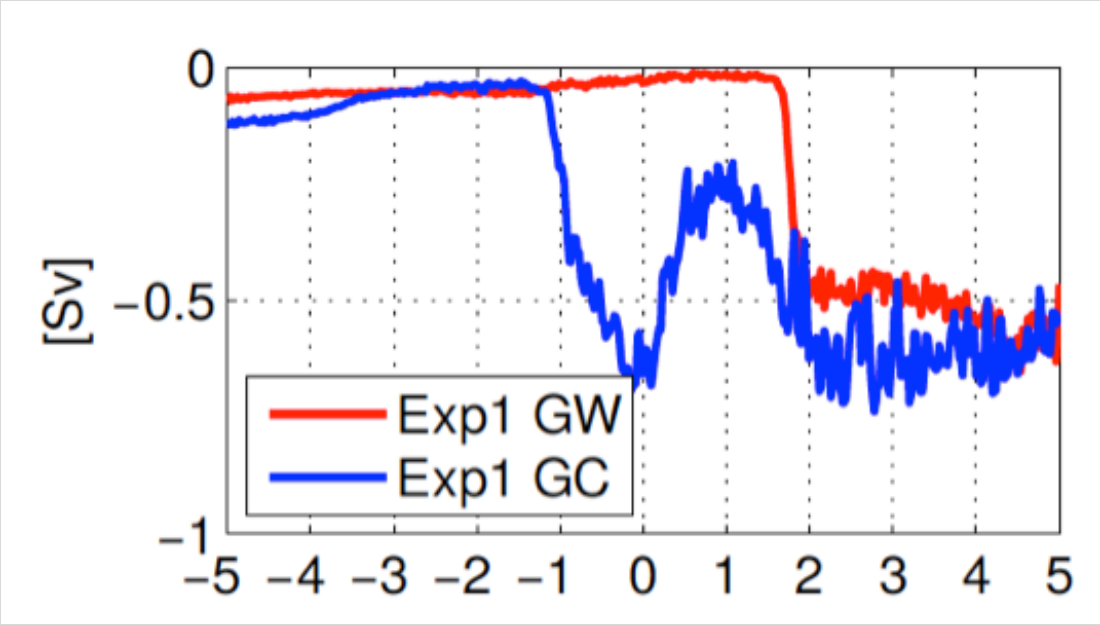

Yael Amitai and
Yossi Ashkenazy

Outline

- Kinematics: Eulerian and Lagrangian viewpoints
- A quick and dirty guide to Lagrangian Coherent Structure and advective chaos
- Applications of Lagrangian dynamics:
    - Barriers to horizontal mixing.
    - Deducing an upper bound to the horizontal eddy diffusivity using a stochastic Lagrangian model.
    - When complexity leads to simplicity: Ocean surface mixing simplified by vertical convection.
    - MET – new diagnostic for LCS
- Conclusions

This lecture will not be an exhaustive treatment; will only introduce basic concepts and few examples.

Kinematics

Dealing with the motion of fluids without considering the forces which create the motion.

Kinematics

Dealing with the motion of fluids without considering the forces which create the motion.

Two methods to observe and analyze fluid flows

Euler

Eulerian viewpoints: observing the velocity and other variables at fixed positions. Most theory of fluid mechanics has been developed in Eulerian systems.

Lagrange

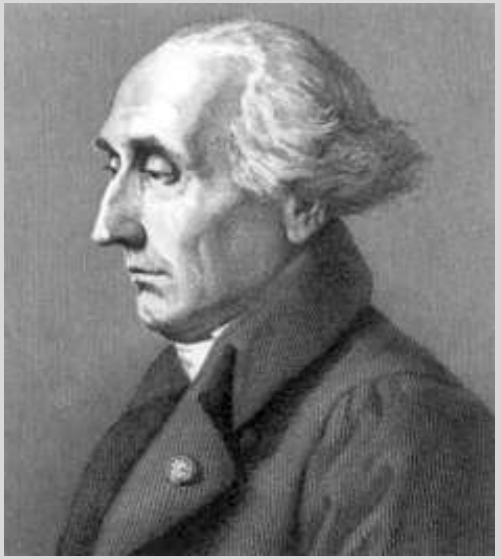

Lagrangian viewpoint: observing the trajectories and velocities of specific fluid parcels. More natural and fundamental.

Think of measuring the temperature with a drifter or a mooring

Lagrangian observations

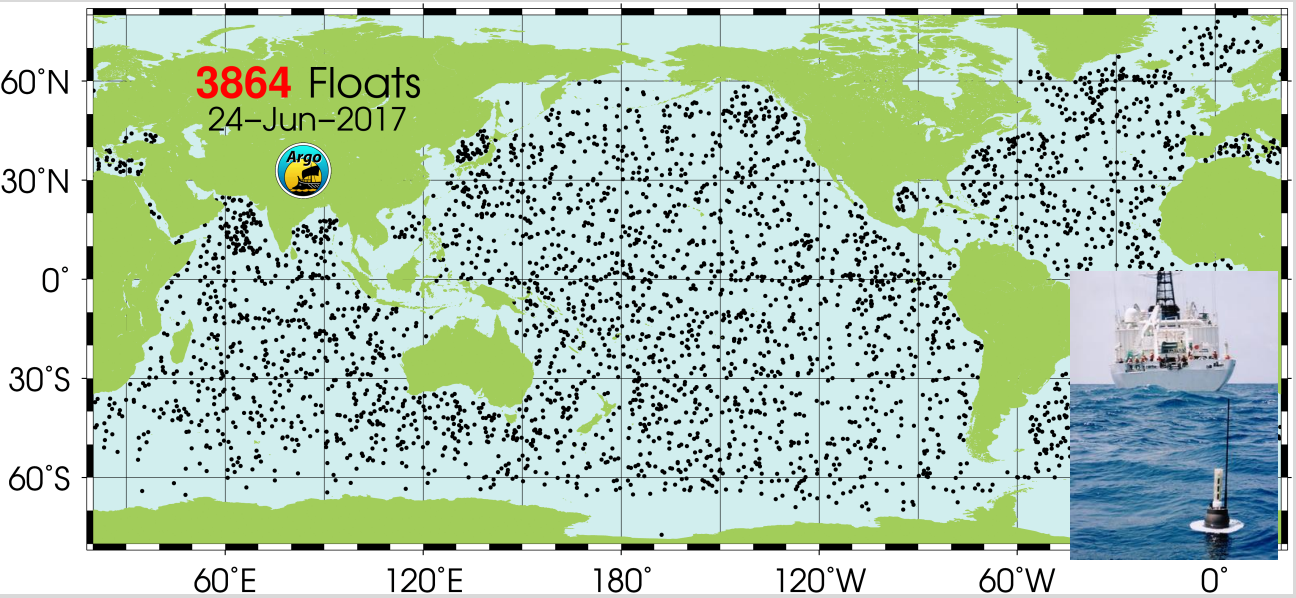

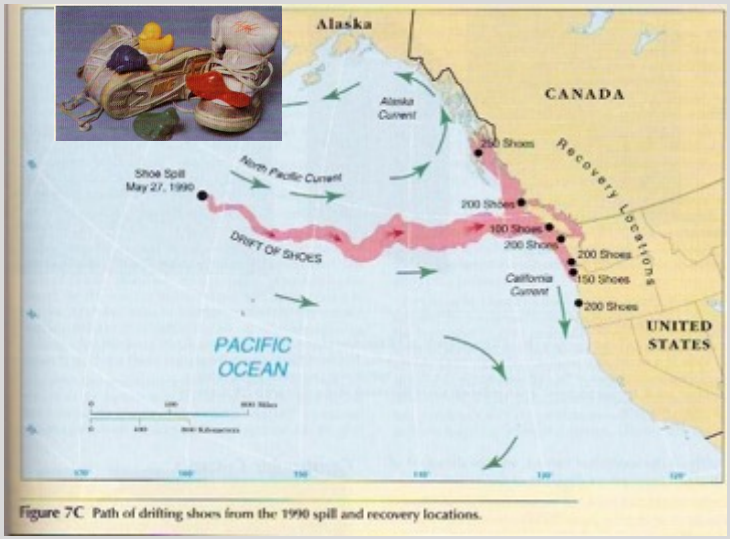

Figure 7C Path of drifting shoes from the 1990 spill and recovery locations.

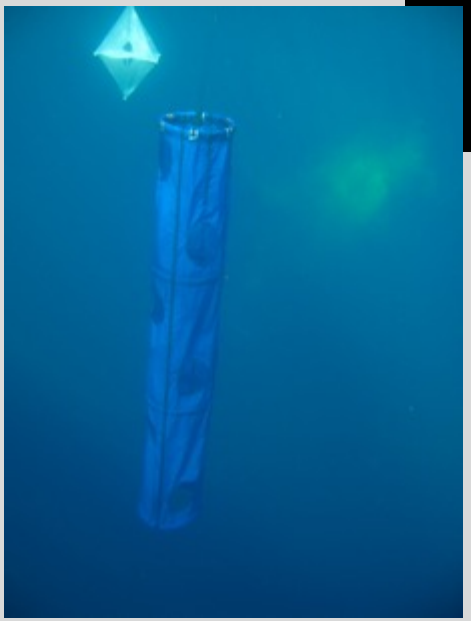

Stommel 1949

Eulerian observations

Mooring

HF radar

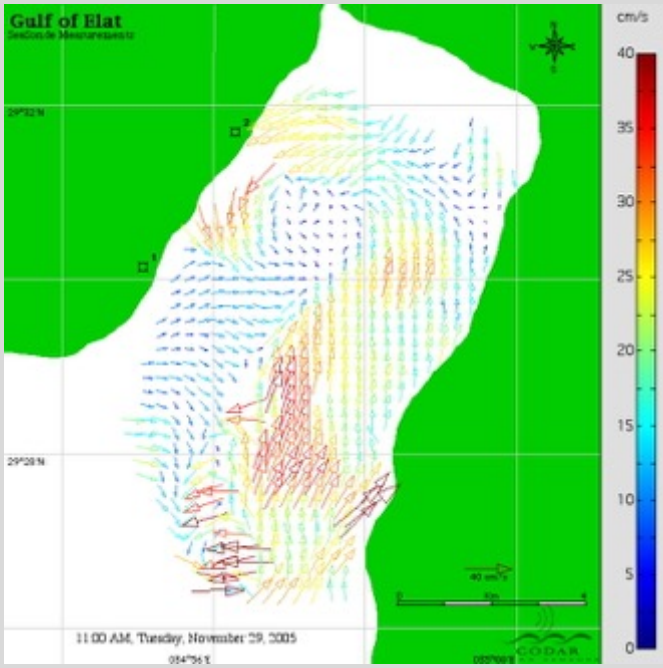

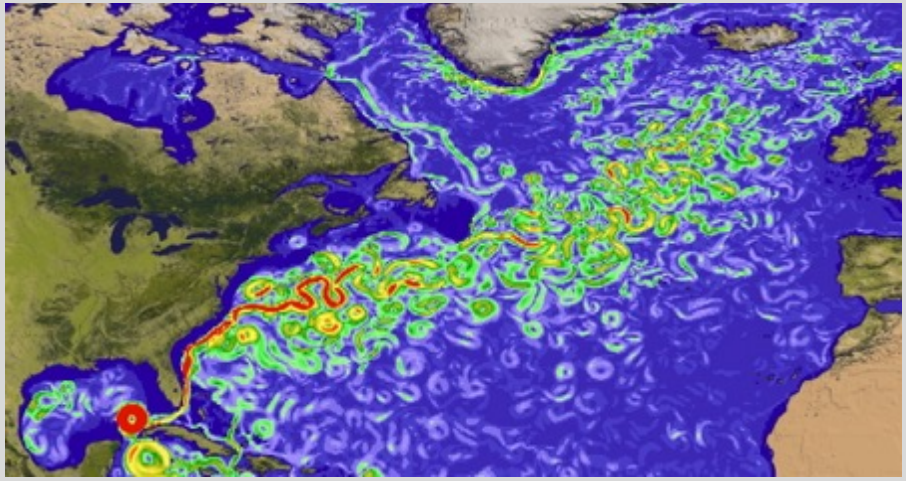

General circulation model

Lagrangian vs. Eulerian

- Fluid mixing is fundamentally a Lagrangian phenomenon. But traditional analysis of mixing was mainly Eulerian. Why?
  - Lagrangian data is hard to obtain. Easier to conduct measurements at a fixed point.
  - Fluid parcels are not well defined. How long can we track a small patch of dye? Too many molecules/parcels.
- Can be done with numerical simulations, HF radars, satellites, and better tools for particle tracking (both in the lab and in the sea).
- Often we use a mixture of Eulerian observations and Lagrangian analysis or vice versa. For examples:
  - Lagrangian trajectories based on velocity field from a numerical model.
  - PIV: Eulerian velocities based on Lagrangian trajectories (successive images of very small, and neutrally buoyant particles).
  - The zeroth order approximation, or PVD (Progressive Vector Diagram).
- Some instruments, e.g. ocean gliders, are neither Eulerian nor Lagrangian.

The advection diffusion equation for an ocean tracer

$$C_t + U(x,t)\cdot\nabla C = D\Delta C$$

- Advection – “bulk” movement; Diffusion – Motion by the molecules.
- Down to small-scales, advection dominant transport.
- There is a coupling between advection and diffusion: advection can increase the gradient of a tracer and this will enhance diffusion.
- Stirring and mixing in a cup of coffee - Eckart 1948

Initial large concentration gradients at the interfaces between globs of coffee and cream, but the interfaces are small in number and of small area.
Stirring: the cream is swirled and folded. The area of the interface and concentration gradients increase.
Mixing: the gradients disappear and the fluid becomes homogenous, due to molecular diffusion.

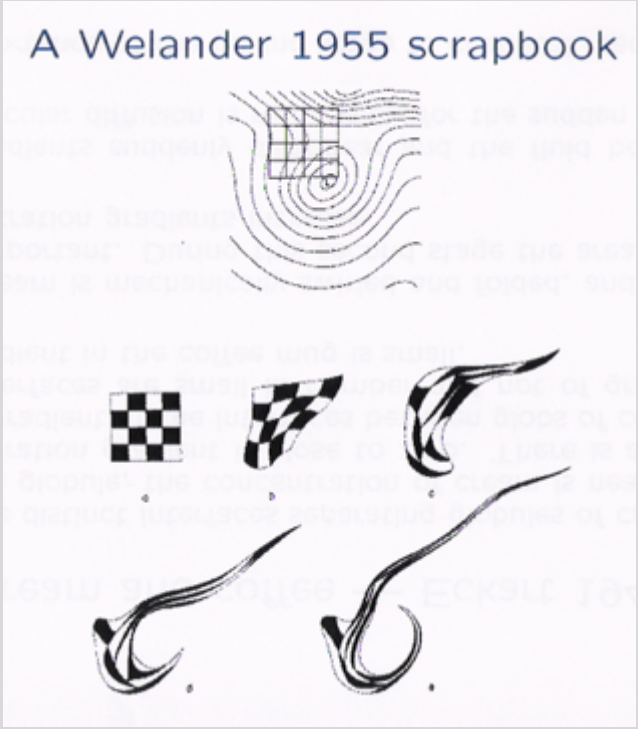

Stirring leads to mixing

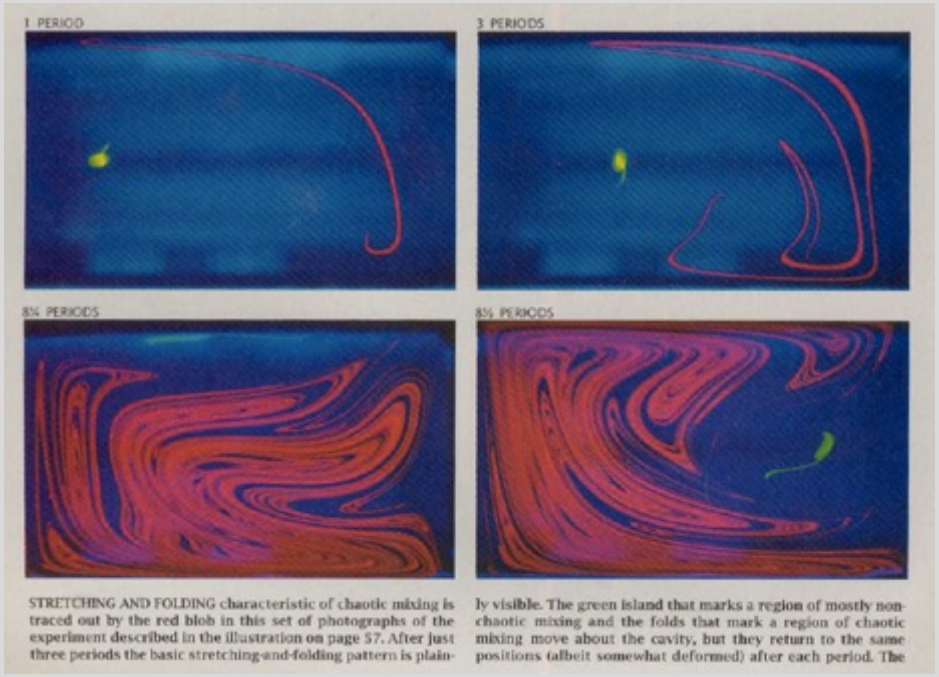

STRETCHING AND FOLDING characteristic of chaotic mixing is traced out by the red blob in this set of photographs of the experiment described in the illustration on page 57. After just three periods the basic stretching-and-folding pattern is plainly visible. The green island that marks a region of mostly nonchaotic mixing and the folds that mark a region of chaotic mixing move about the cavity, but they return to the same positions (albeit somewhat deformed) after each period. The

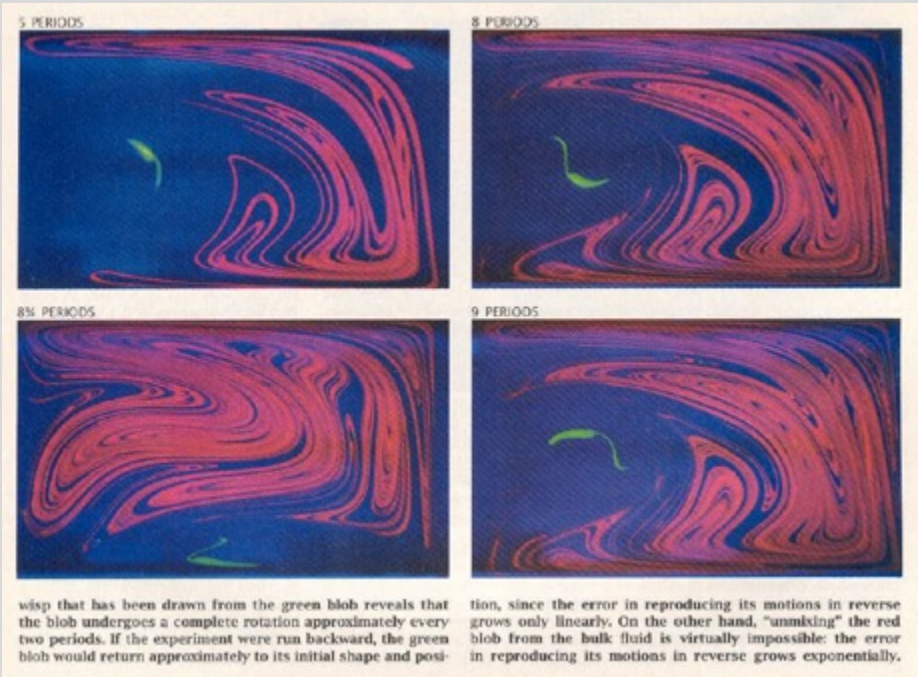

wisp that has been drawn from the green blob reveals that the blob undergoes a complete rotation approximately every two periods. If the experiment were run backward, the green blob would return approximately to its initial shape and position, since the error in reproducing its motions in reverse grows only linearly. On the other hand, "unmixing" the red blob from the bulk fluid is virtually impossible: the error in reproducing its motions in reverse grows exponentially.

Ottino, Sci. Am., 1989

Building blocks:

Parabolic points – shear

Elliptic points – centers

Hyperbolic (saddle) points

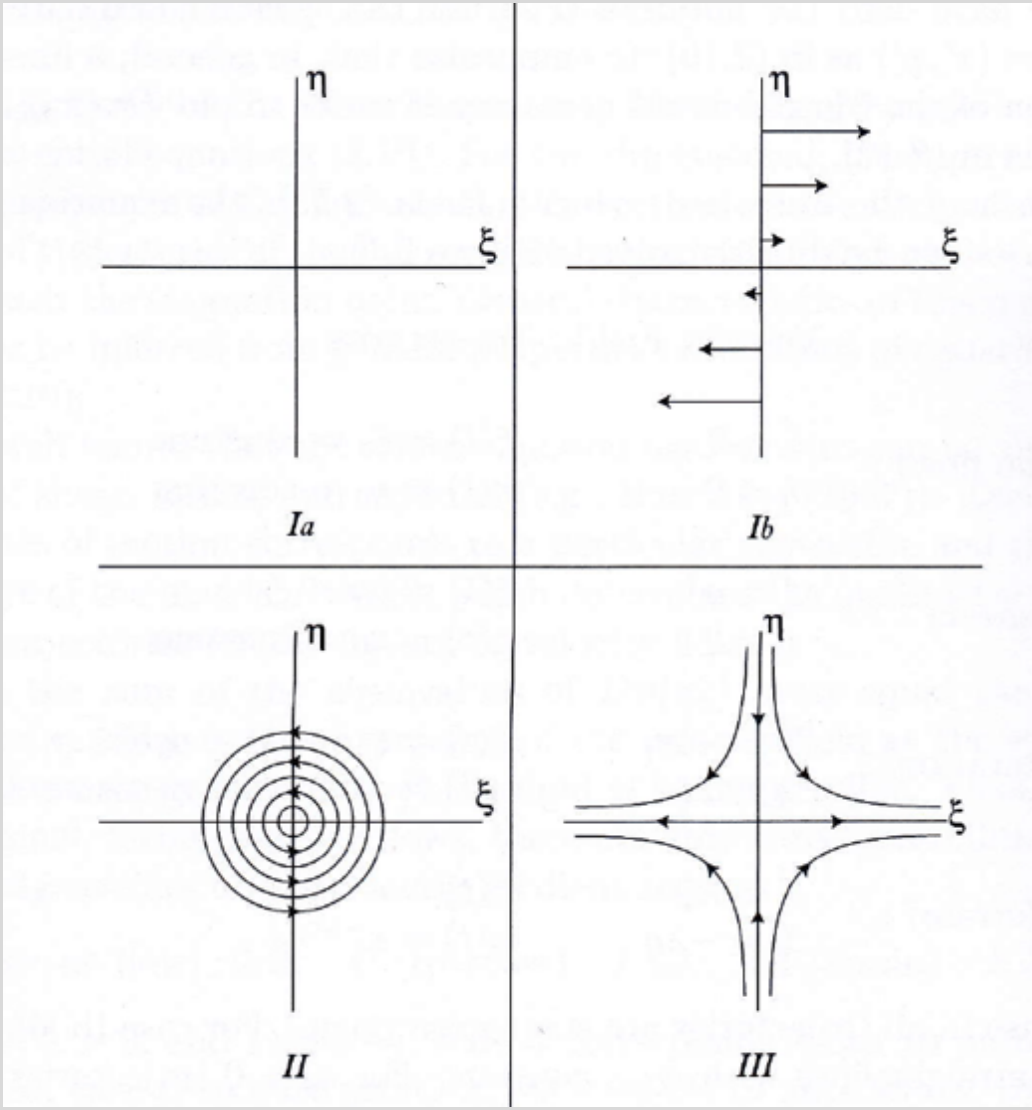

Unstable and stable manifolds

Unstable (stable) manifolds are material lines with diverging (converging), transverse dynamics.

Unstable – collection of all initial particles that asymptote for $t \to -\infty$

Stable – asymptotic for $t \to \infty$

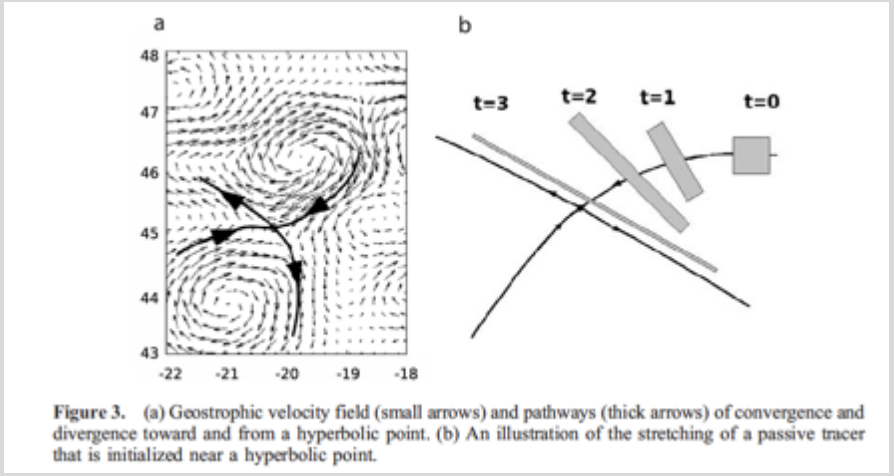

Figure 3. (a) Geostrophic velocity field (small arrows) and pathways (thick arrows) of convergence and divergence toward and from a hyperbolic point. (b) An illustration of the stretching of a passive tracer that is initialized near a hyperbolic point.

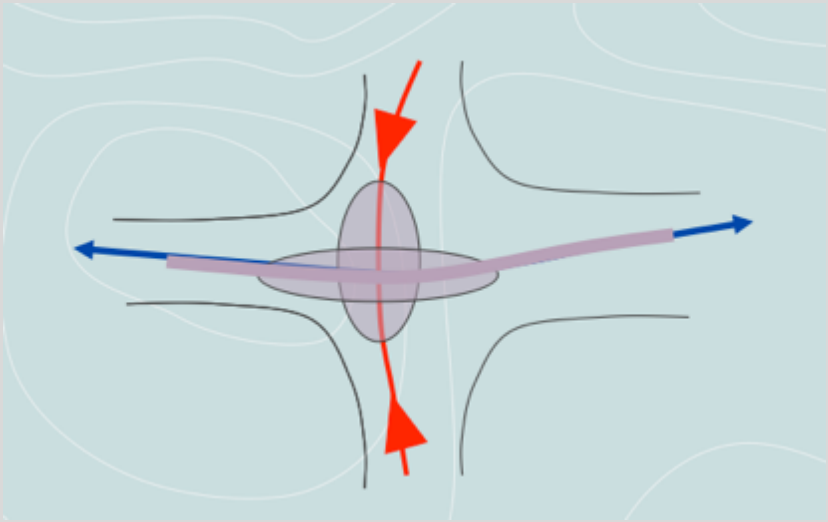

Lehahn et al., 2007

From Rom-Kedar

They form a transport barrier.

Unstable and stable manifolds

Unstable manifold “attracts” passive scalars: **The unstable manifold is the observable structure in many (geophysical and other) flow visualizations.**

LCS: generalization of unstable manifolds to “attracting material line” for real data applications finite times (not periodic), finite resolution, noise (Haller et al., 2002).

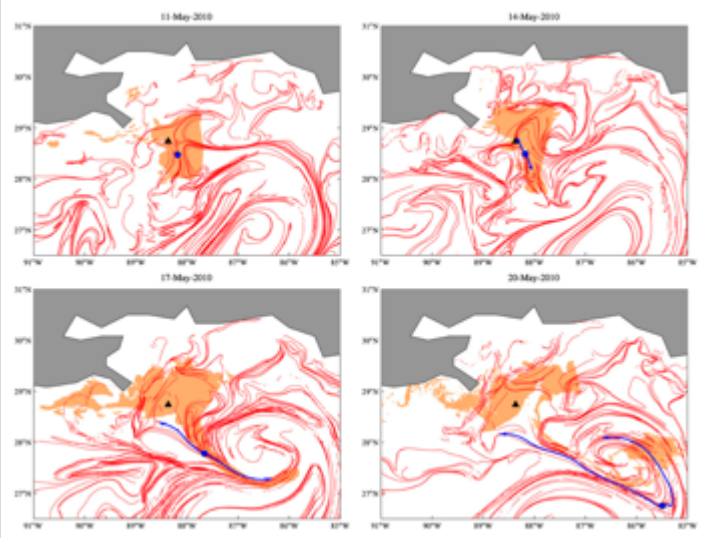

LCS and oil spills, Olascoaga and Haller, PNAS 2012

Fig. 4. (Color online.) Filamentation in a phytoplankton bloom in the Norwegian Sea. Provided by the SeaWiFS Project, NASA/Goddard Space Flight Center, and ORBIMAGE. URL: http://visibleearth.nasa.gov/cgi-bin/viewrecord?5279.

Tel et al., 2005: Phytoplankton bloom in the Norwegian Sea, SeaWiFs

Unstable and stable manifolds

Unstable manifold "attracts" passive scalars: **The unstable manifold is the observable structure in many flow visualizations.**

LCS: generalization of unstable manifolds to "attracting material line" for real data applications finite times (not periodic), finite resolution, noise (Haller et al., 2002).

Oceanic coherent structures: western boundary currents, eddies, jets, … often between counter rotating eddies.

Various technique to identify (FTLE, FSLE, Relative dispersion, MET, …).

The stable and unstable manifolds tangle governs the transport.

Stationary double gyre model

Velocities are derived from a stream-function

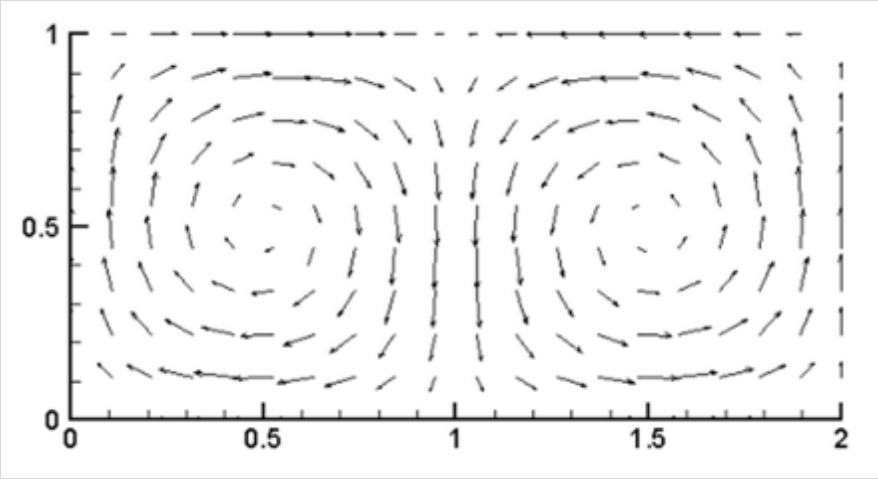

Steady velocity fields cannot (usually) give rise to complicated mixing (Arnold, 65)

Flow characteristics often change near stagnation points

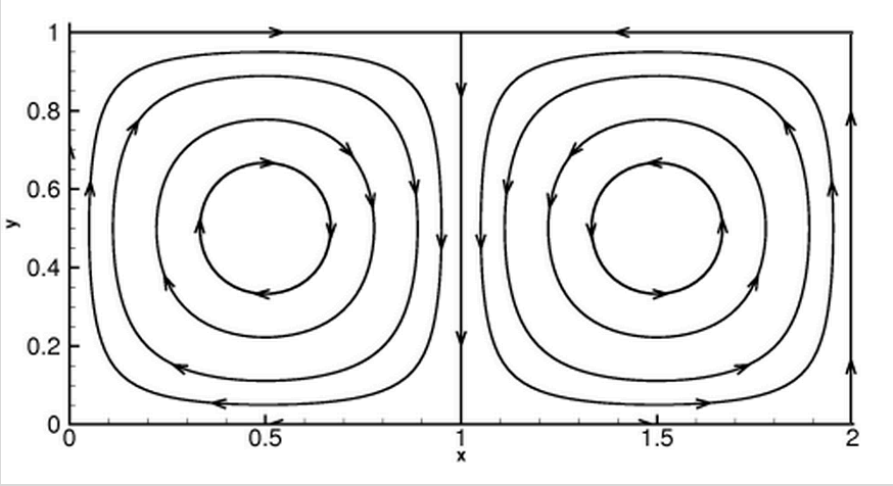

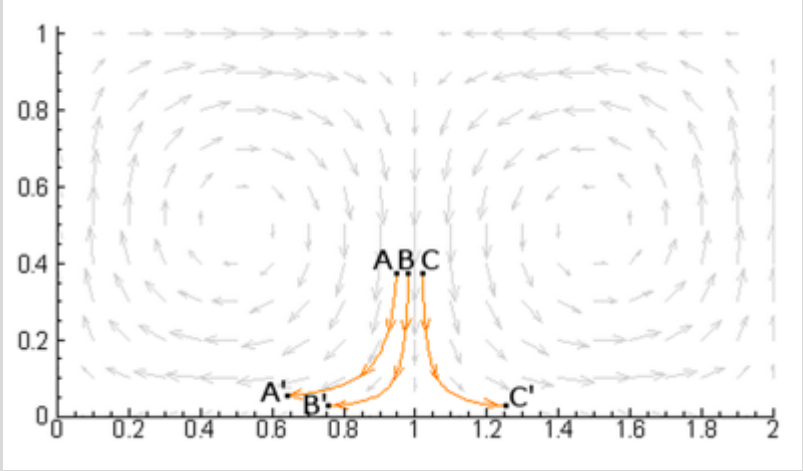

http://www.cds.caltech.edu/~shawn/LCS-tutorial/contents.html

Time dependent (tide?) double gyre

Chaotic advection

Advective chaos (mixing) can exist even when the velocity fields seem smooth and regular (low-Reynold number, no turbulence)

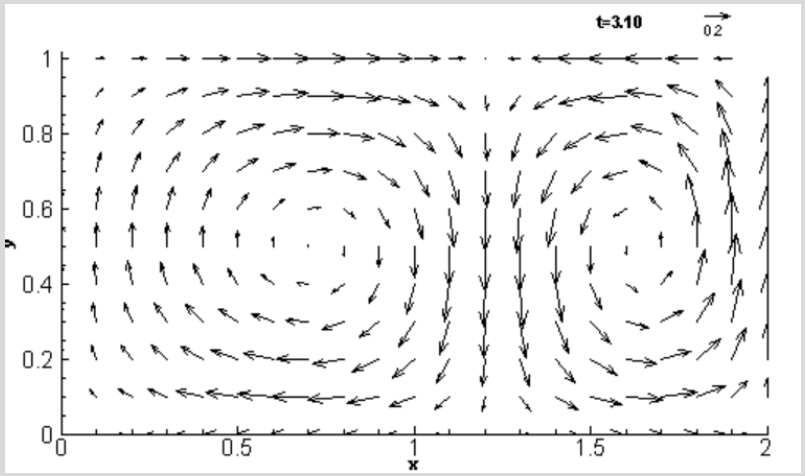

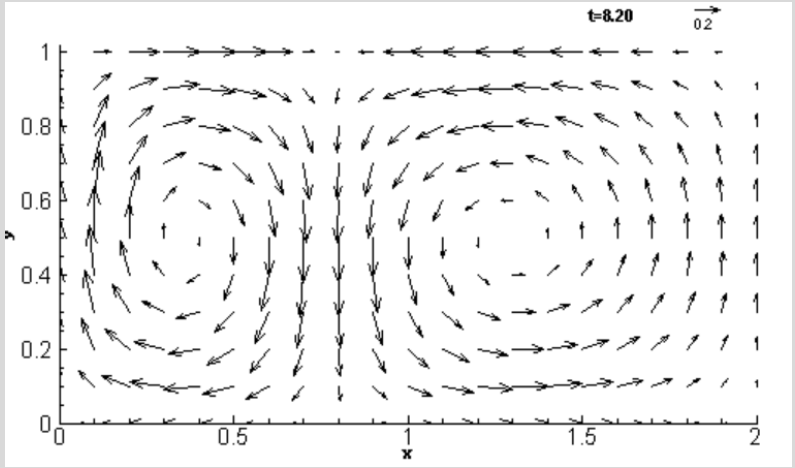

LCS

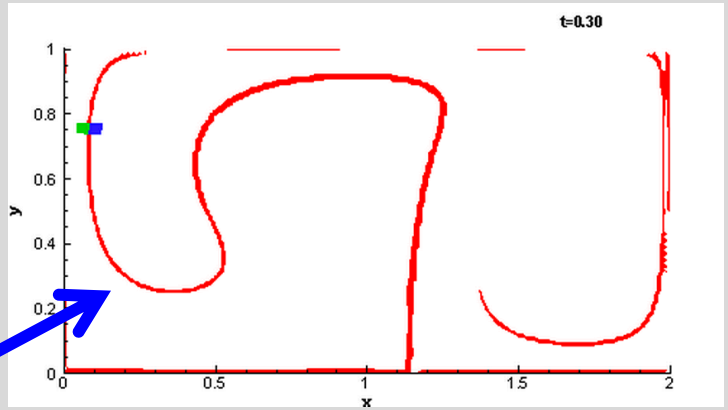

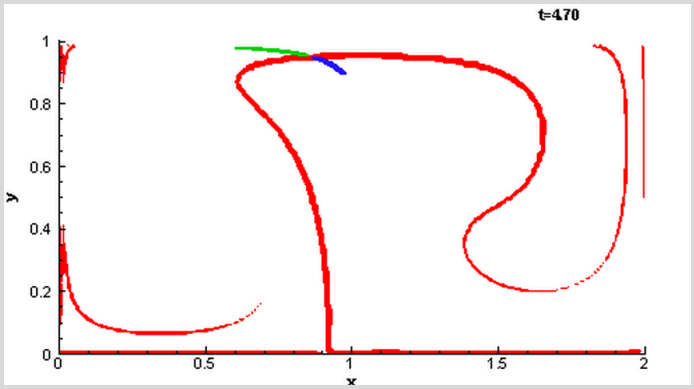

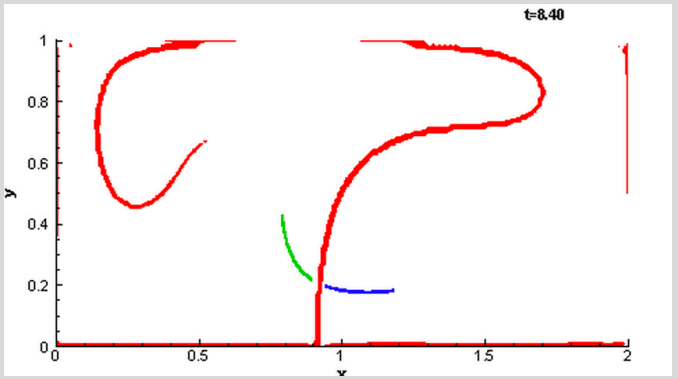

http://www.cds.caltech.edu/~shawn/LCS-tutorial/contents.html

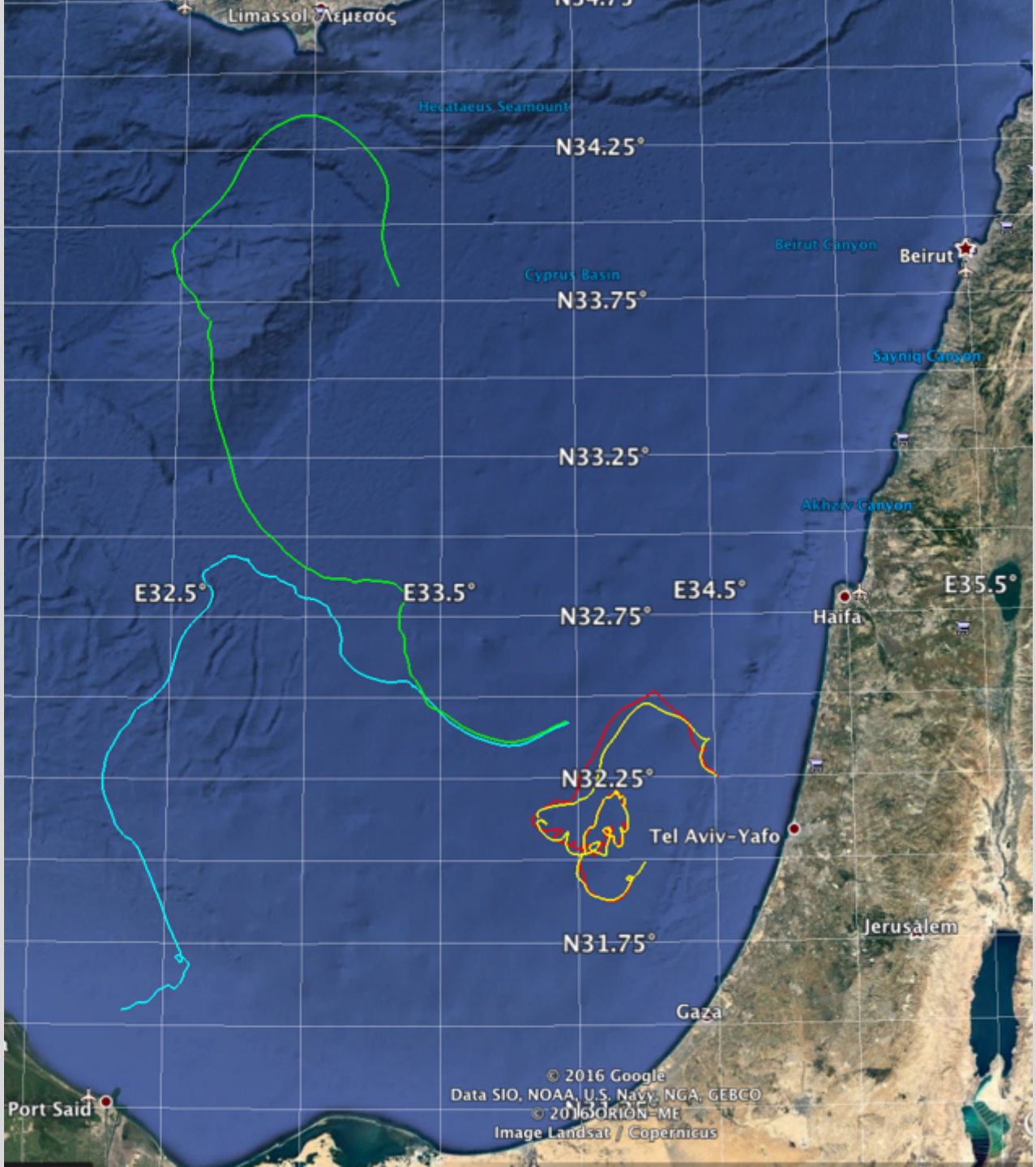
Limassol Λεμεσός
Hecataeus Seamount
N34.25°
Beirut Canyon
Beirut
Cyprus Basin
N33.75°
Sayniq Canyon
N33.25°
Akhziv Canyon
E32.5°
E33.5°
E34.5°
E35.5°
N32.75°
Haifa
N32.25°
Tel Aviv-Yafo
Jerusalem
N31.75°
Gaza
Port Said
© 2016 Google
Data SIO, NOAA, U.S. Navy, NGA, GEBCO
© 2016 ORION-ME
Image Landsat / Copernicus

OGS, OS-UCY

Why statistics over many particles?

- Chaotic system-> sensitivity to initial conditions-> we should average over many particles
- Single particles statistics (mean, PDFs, diffusivities, …)
- Multiple particles statistics

Single particle dispersion: Describes the spreading process

$$A_k^2(t,t_0) = \{\vec{X}_k(t) - \vec{X}_k(t_0)\}^2$$

Two particles Relative Dispersion

To understand spatial correlations we must examine at least pairs of particles

$$RD_k^2(t,t_0) = \frac{1}{4}\sum_{j=1}^{4}\{\vec{X}_j(t) - \vec{X}_k(t_0)\}^2$$

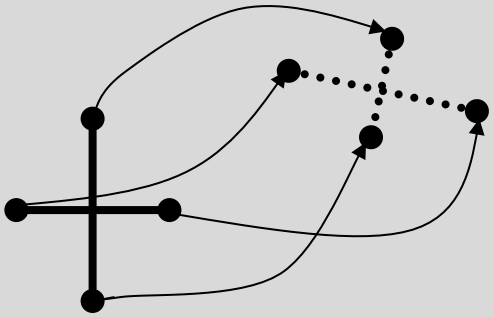

Lyapunov exponents

$$r_k(t) \cong r_k(0)e^{\lambda t}$$

Ridges of RD represents LCS
(and barriers to mixing)

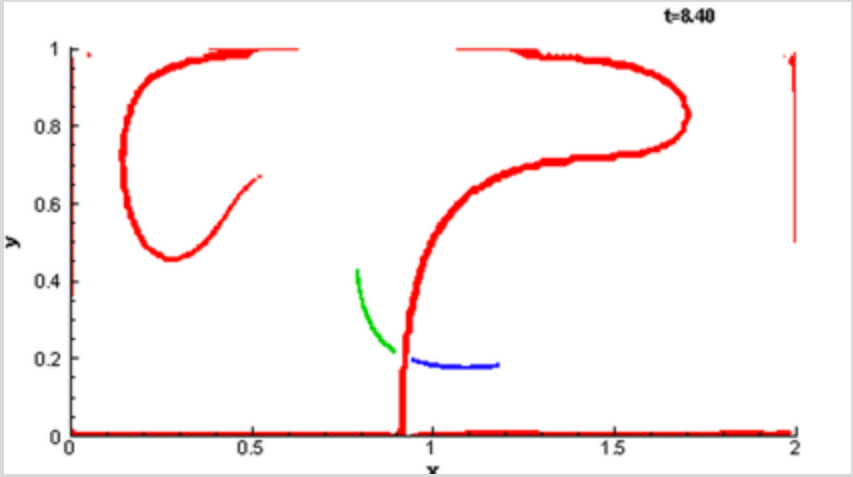

Applications for Lagrangian studies

Mixing problems: from micro mixers through traditional lab-scales/mechanics to geophysics (see reviews by T. Tel (2006), Ottino & Wiggins (2004),.., Prants (2013)):

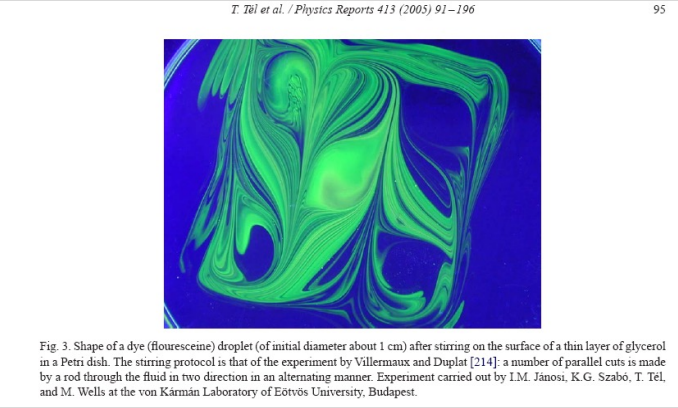

Fig. 3. Shape of a dye (flouresceine) droplet (of initial diameter about 1 cm) after stirring on the surface of a thin layer of glycerol in a Petri dish. The stirring protocol is that of the experiment by Villermaux and Duplat [214]: a number of parallel cuts is made by a rod through the fluid in two direction in an alternating manner. Experiment carried out by I.M. Jánosi, K.G. Szabó, T. Tél, and M. Wells at the von Kármán Laboratory of Eötvös University, Budapest.

Petri dish mixing Janosi et al. 2007

What does it mean to "characterize mixing"?

Given **u**(x,t), identifying:

1) Coherent structures
2) Dividing structures
3) Mixing layers

Applications for Lagrangian studies

Ocean Mixing: a fundamental problem of theoretical interest (how to characterize the mixing, parameterized mixing, extract LCS, …) and with many practical applications.

- Oil spills
- Connectivity
- Search and rescue
- Identifying source regions
- Minimize pollution

Deepwater Horizon Oil Spill

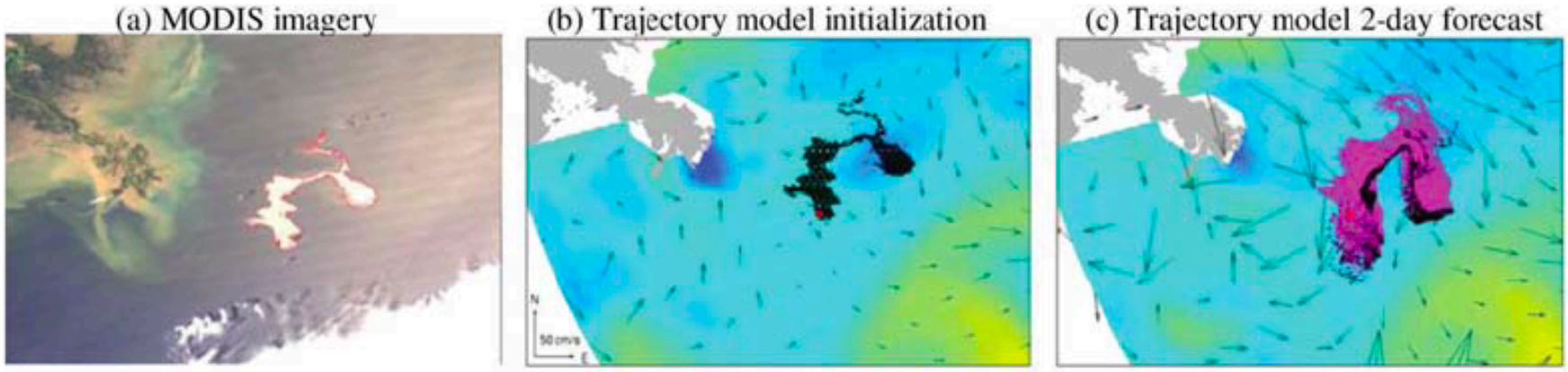

Figure 2. Illustration of the re-initialization of the surface trajectory analyses based on the West Florida Shelf (WFS) circulation model: (a) surface oil slick inferred from MODIS satellite imagery on 18:55 UTC, 25 April 2011 (outlined in red); (b) virtual particles seeded at the locations covered by the satellite-derived surface oil slick; (c) trajectory forecast 2 days after the initialization. Black denotes virtual drifters; purple denotes areas swept out by virtual drifters. Background fields are instantaneous sea surface temperature (SST) and surface currents. This figure is adapted from the work of *Liu et al.* [2011b].

Connectivity

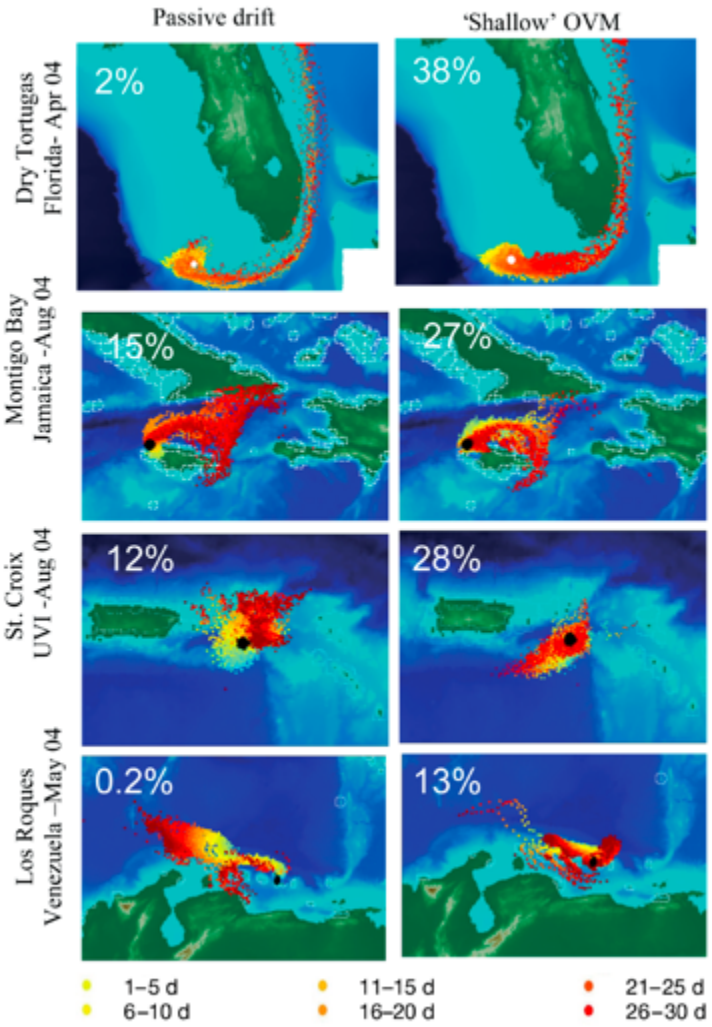

Fig. 11. Influence of larval behavior on dispersal: 30 d passive dispersal snapshots from various locations in the Caribbean are compared to dispersal with 'shallow' ontogenetic vertical migration (OVM) of the bicolor damselfish *Stegastes partitus*. Percent of simulated larvae arriving onto any reef is indicated

Search and Rescue

Ocean Dynamics
DOI 10.1007/s10236-012-0546-4

Backtracking drifting objects using surface currents from high-frequency (HF) radar technology

Ana Julia Abascal · Sonia Castanedo · Vicente Fernández · Raúl Medina

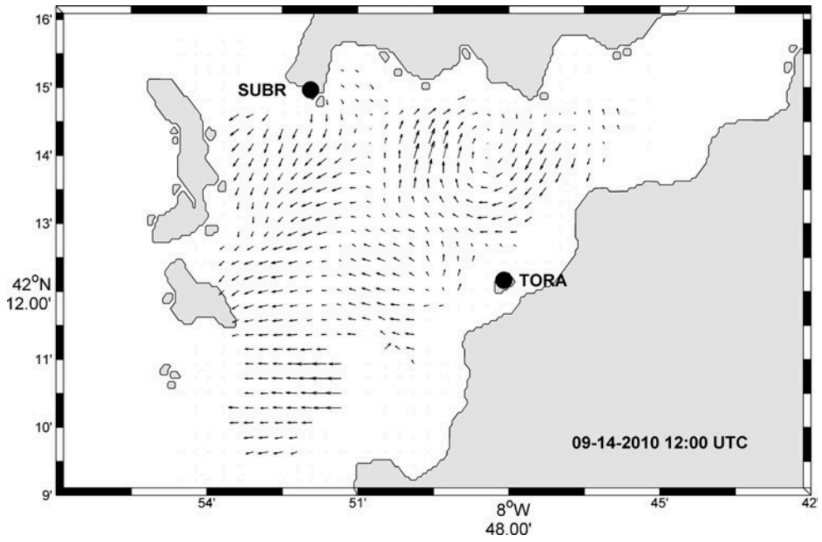

Fig. 3 Typical surface current map provided by the high-resolution Bay of Vigo coastal HF radar system of the University of Vigo. The radar site locations are indicated by *solid black circles*

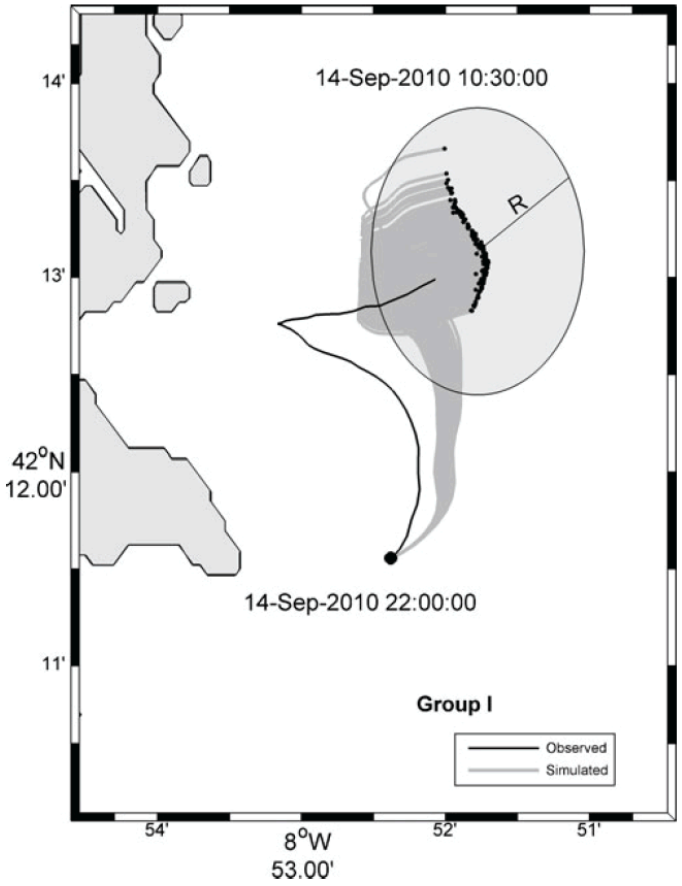

Fig. 15 Search area (*grey circle*) to find the origin of buoy number 1 (group I) in the first period (R=1.01 km). Actual and simulated backward trajectories are indicated by *black* and *grey lines*. The buoy trajectory spans from September 14 10:30 UTC to September 14 22:00 UTC. The initial time and position of the simulation is indicated by the black circle. The *black dots* stand for the final position of the backtracked trajectories

Other applications

- Identifying source regions

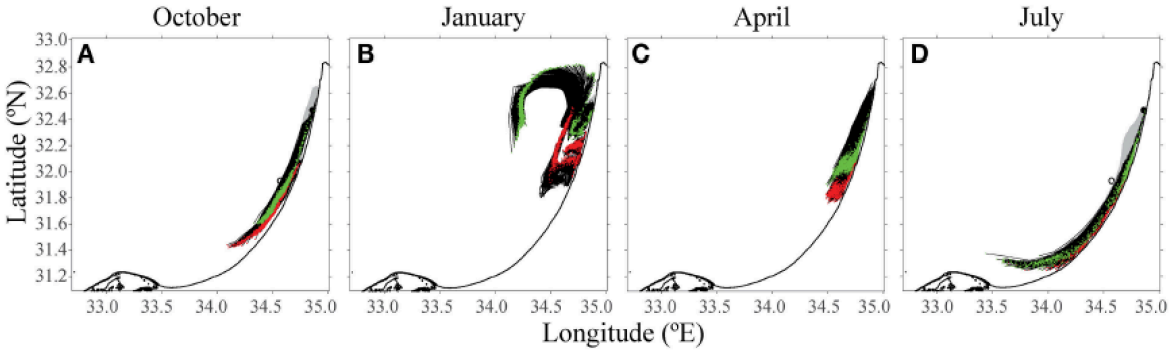

FIGURE 8 | Results from the 15-day back-trajectories analysis to source water origins from the desalination plant and the public beach. The green path indicates particles from Hadera desalination factory target, and the red path follows water sampled from a Tel Aviv public beach. Both the black and gray are the trajectories of the particles till the target. The open circle is the location of the existing fish farm cages offshore Ashdod. **(A)** October, **(B)** January, **(C)** April, and **(D)** July.

Grossowicz et al., 2017

- Minimize pollution

Lekien et al., 2005

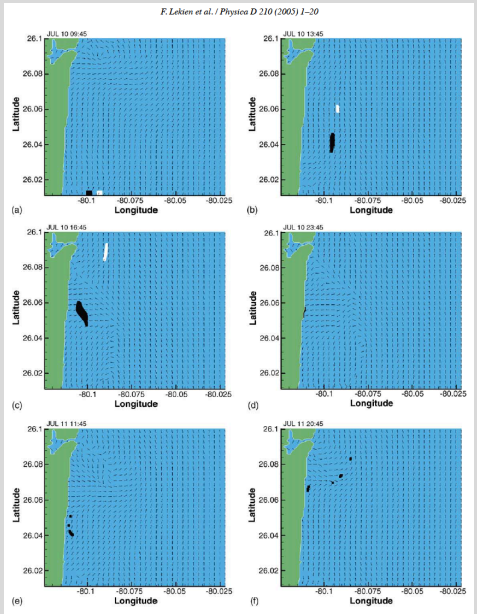

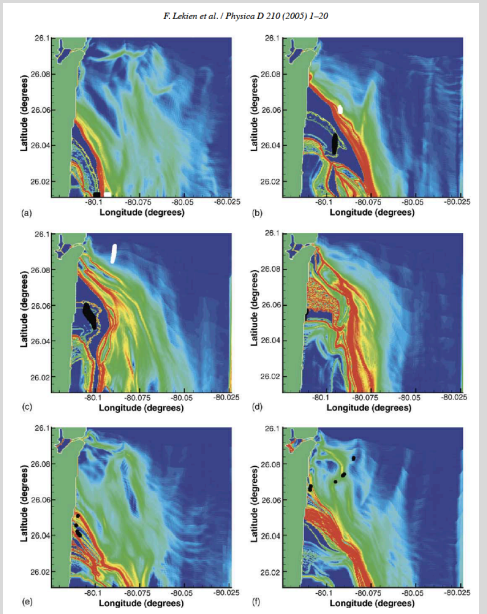

- Project Home
- Daily Analysis

Spacial Focus:

- Waste deposition on the coast of Israel
- In situ observations

About the system:

- Satellite Data
- SELIPS model
- Lagrangian Analysis
- References
- Contacts List

Lagrangian Analysis of Passive Tracer Circulation

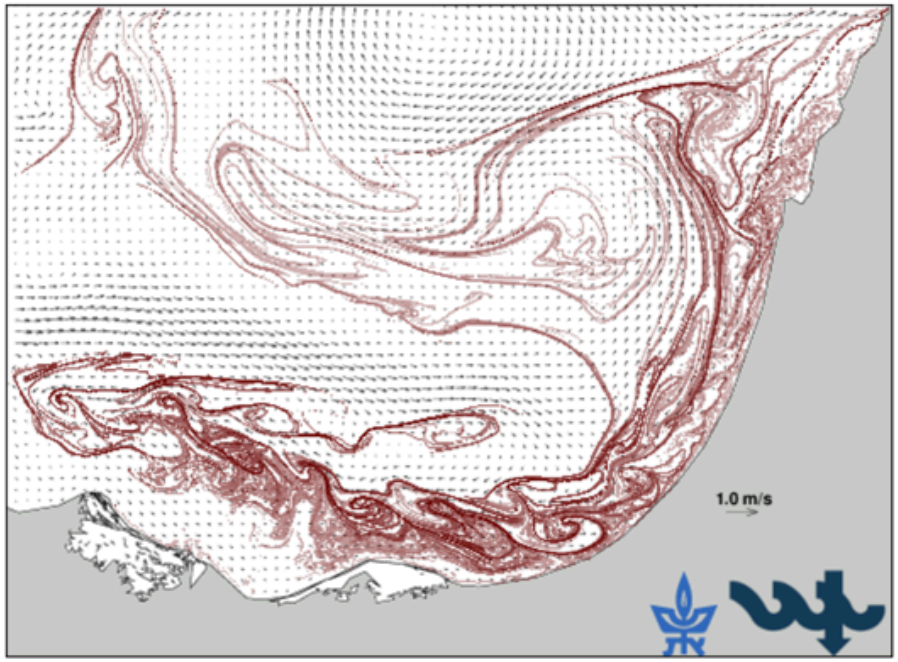

Select Procut and Time:

SELIPS

|< < 2017-01-26 > >|

Animate

Show:

- Chlorophyll a Case1-Case2 Generated using Copernicus products [?]
- SELIPS daily averaged currents [?]
- Finite Size Lyaponov Exponent
  - *Unstable* *Stable* [?]

About the project

http://isramar.ocean.org.il/isramar2009/cosem/fsle.aspx

From Isramar web site:

Calculating Lagrangian trajectories

- Acquire the velocity field (numerical model, HF radar, satellite altimetry…)
- Choose the particle tracking model:
  - Simple deterministic tracking model (passive tracers); Ignore model/measurement errors, subgrid processes; Inertia-less particles; no interaction.

$$\frac{dx_n}{dt} = u(x_n, y_n, t), \frac{dy_n}{dt} = v(x_n, y_n, t)$$

  - 1st order stochastic model.
  - Individual based model (coupling dynamics and behavior). Swimming, e.g., can have significant effects.
  - Numerical considerations: numerical scheme, time step, interpolation of the velocity field

Barriers to horizontal mixing in the Gulf of Eilat

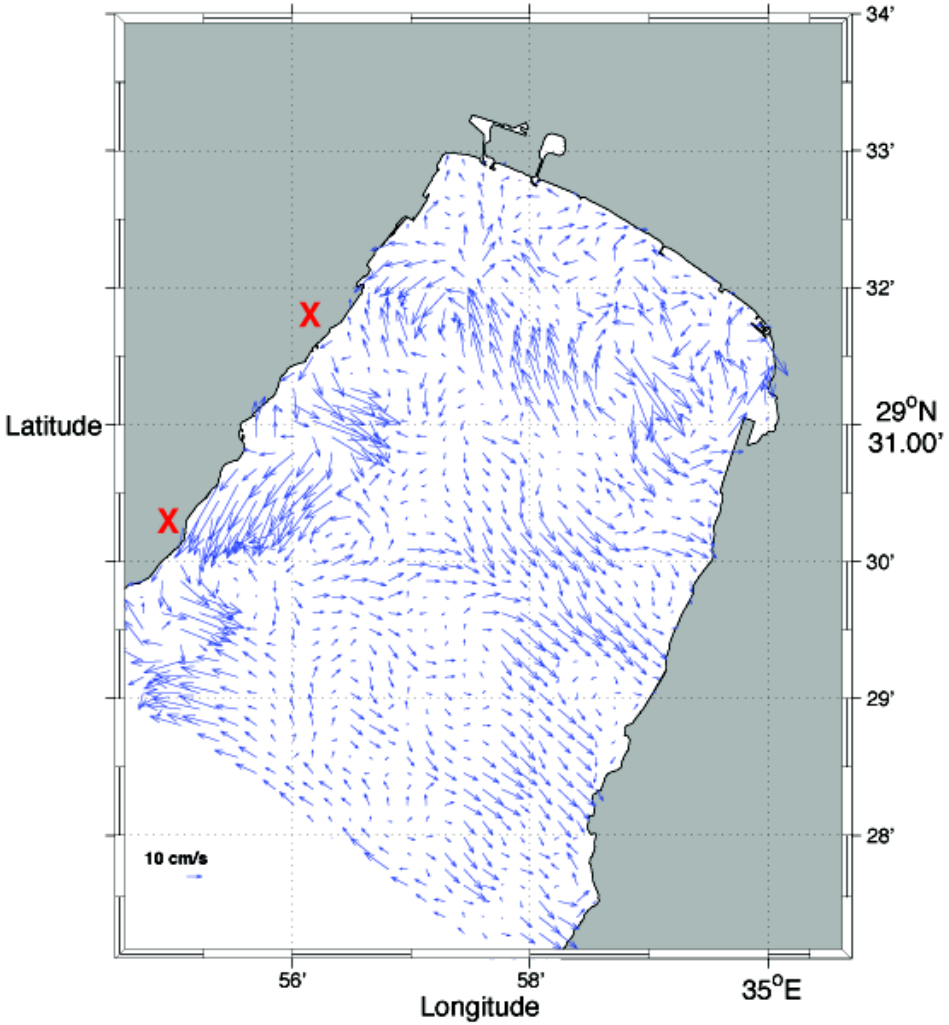

HF radar enables to observe ocean currents at *unprecedented spatial & temporal resolutions*

Flow field seems energetic and complex.

Typical speed - 15 cm/s

Dominant tidal cycle - M2

Expect full mixing within a day or two.

Results of Lagrangian particle calculation: Relative dispersion after 36 hours, 2-4 Feb, 2006

Local high relative dispersion along bright lines

Overall: very non uniform dispersion

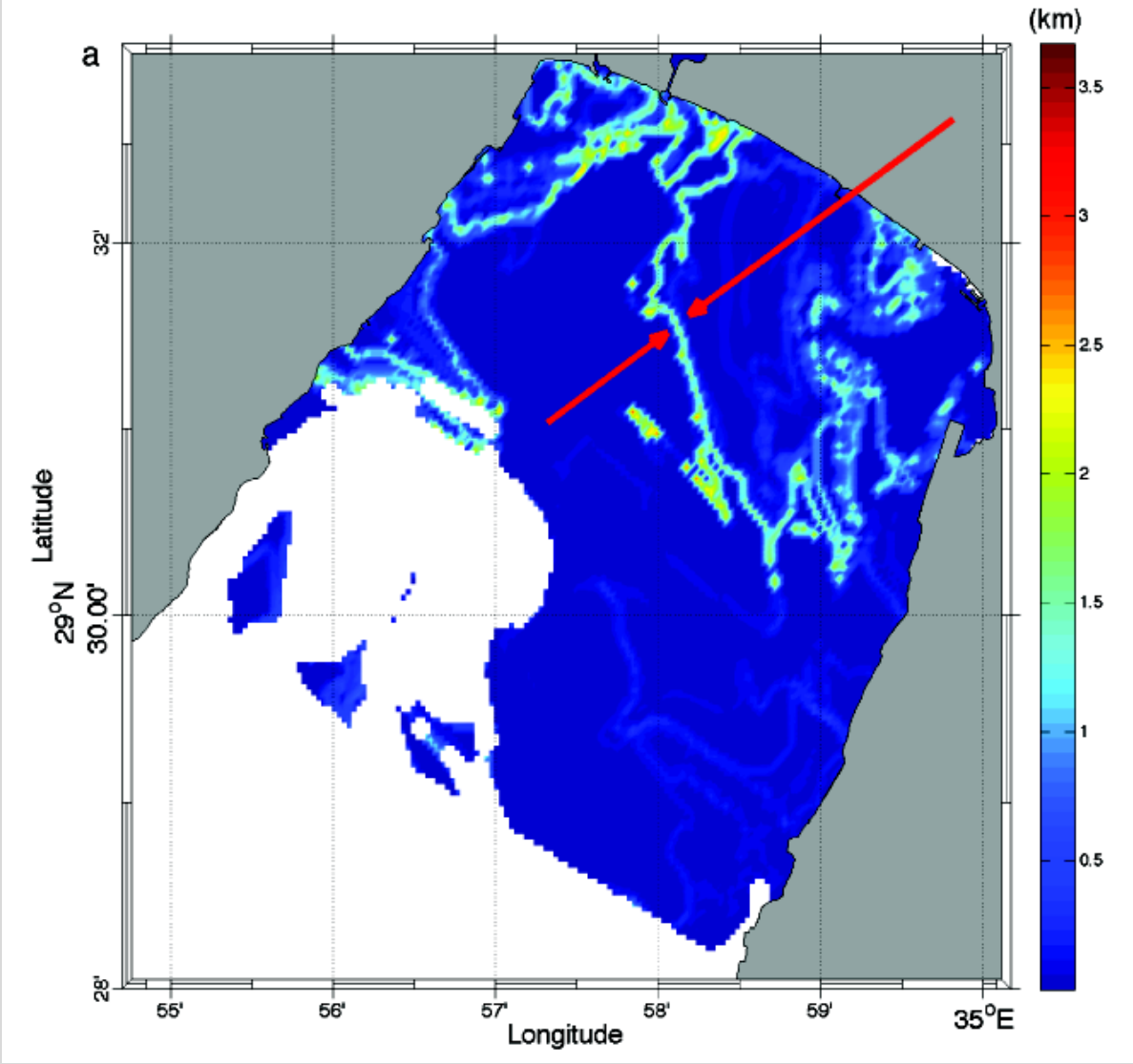

Aerial photographs showing the existence of persisting barriers to mixing

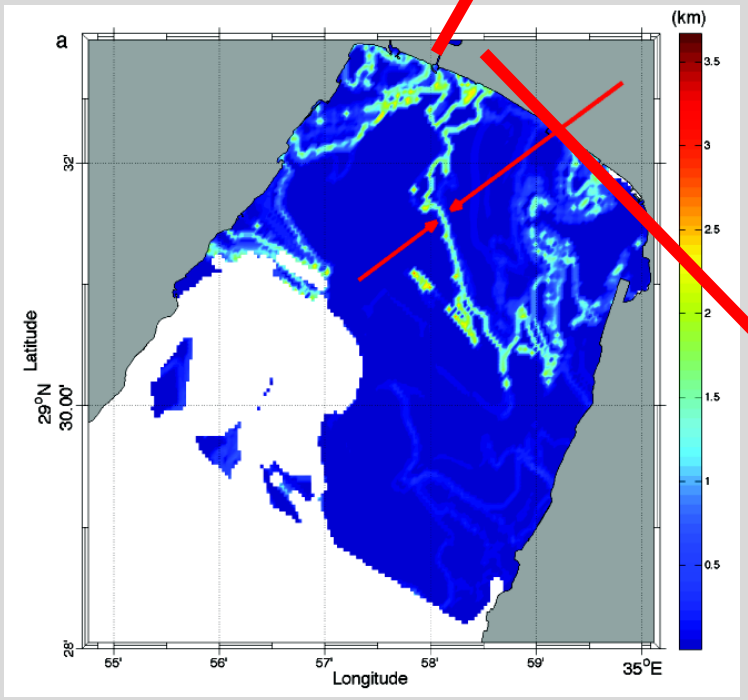

Feb. 3, 2006

Aerial photographs: persisting barriers to mixing

After two days, Feb. 5, 2006

Spatial variations of the relative dispersion and the Lyapunov exponents seem to explain the observed sharp front. This implies non-uniform mixing, unlike what most models use …

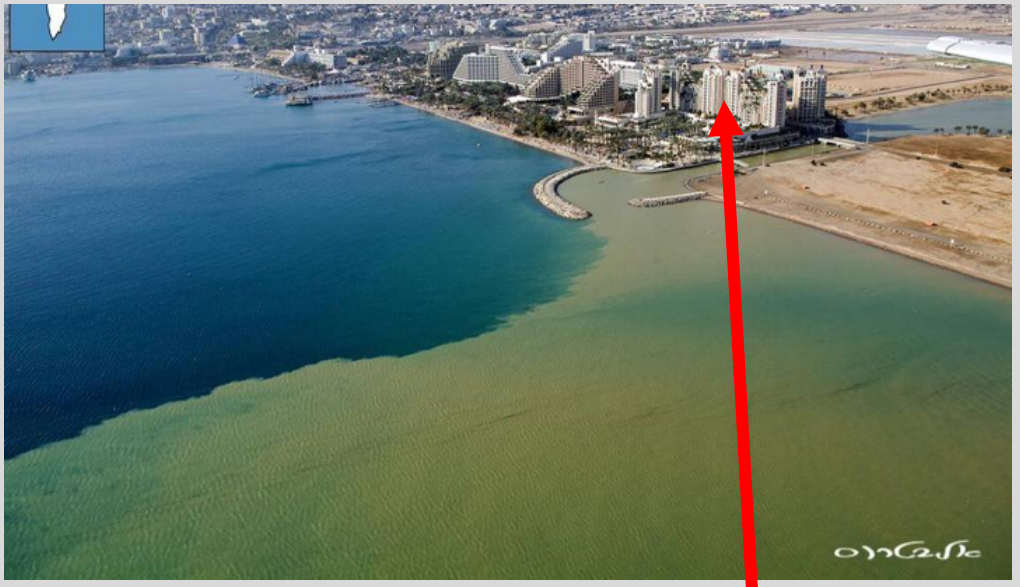

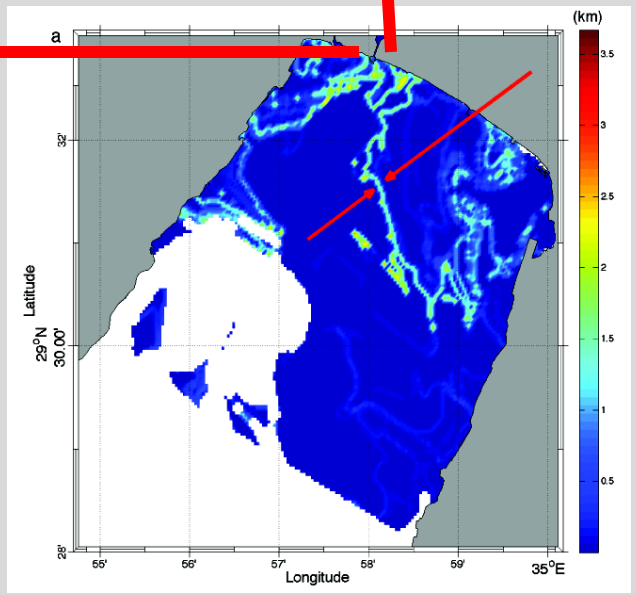

Conclusions I:
horizontal submesoscal barriers to mixing

1. Tracer transport is *not homogenous and isotropic*; unexpected complexity and variability, *submesoscale barriers to mixing.*
2. Such a barrier, when present, can trap passive tracers such as larvae or pollutants. Barriers prevent potential vorticity mixing as well??
3. Submesoscale turbulence is characterized by non-Gaussian velocity distribution.
4. (2,3,4): incompatible with GCM eddy parameterizations.

JPO, 2009; *JGR*, 2009a; *JGR*, 2009b; *JPO*, 2011

Environ Fluid Mech
DOI 10.1007/s10652-010-9181-0

ORIGINAL ARTICLE

Deducing an upper bound to the horizontal eddy diffusivity using a stochastic Lagrangian model

Daniel F. Carlson · Erick Fredj · Hezi Gildor · Vered Rom-Kedar

Recipe

♣ Identify a mixing barrier from a priori evidence (e.g., aerial photographs or satellite imagery).

Gildor et al., *J. Phys. Oceanogr.,* 2009.

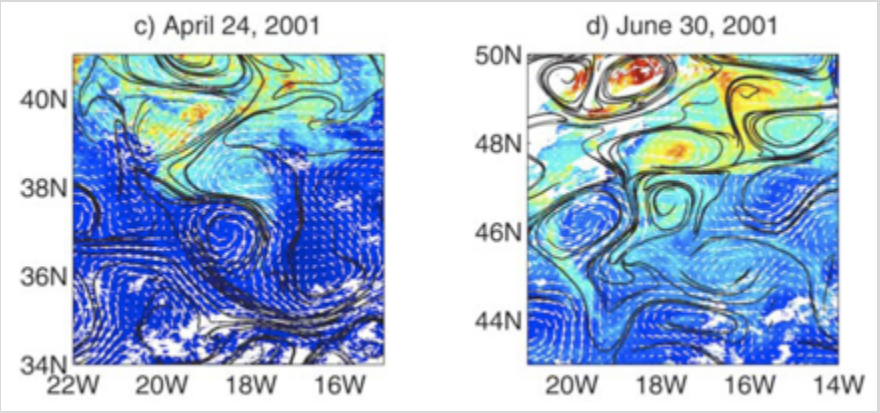

Lehahn et al., *J. Geophys. Res.*, 2007.

Recipe

- ♣ Identify a mixing barrier from a priori evidence (e.g., aerial photographs or satellite imagery).
- ♣ Establish the existence of the barrier by calculating a Lagrangian diagnostic such as relative dispersion (RD) of passive particles advected by the observed spatially non trivial, *time-dependent* velocity field.

$$dX(t) = \mathbf{U}_{LS}\left(\mathbf{X}(t), t\right)dt$$

- ♣ Add a stochastic component, representing eddy diffusivity, when calculating the particles trajectories (zeroth-order stochastic model).

$$dX(t) = \mathbf{U}_{LS}\left(\mathbf{X}(t), t\right)dt + \sqrt{2K}\,dw(t)\,dt$$

- ♣ Increase the eddy diffusivity until the mixing barrier disappears. The value at which the barrier disappears provides an estimation of the upper bound for the eddy diffusivity.

Toy model demonstration: Time dependent double gyre

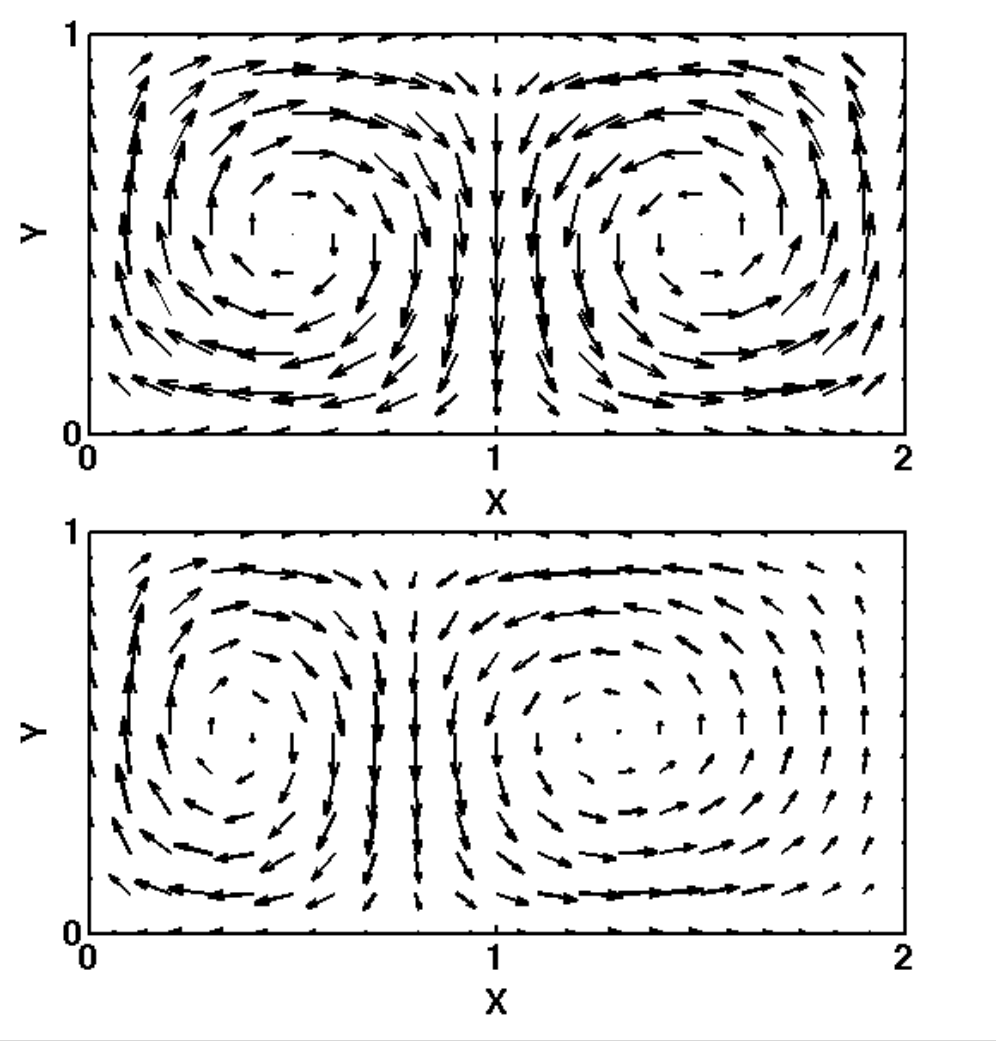

Velocities are derived from a stream-function.

http://www.cds.caltech.edu/~shawn/LCS-tutorial/contents.html

Time-dependent double gyre model

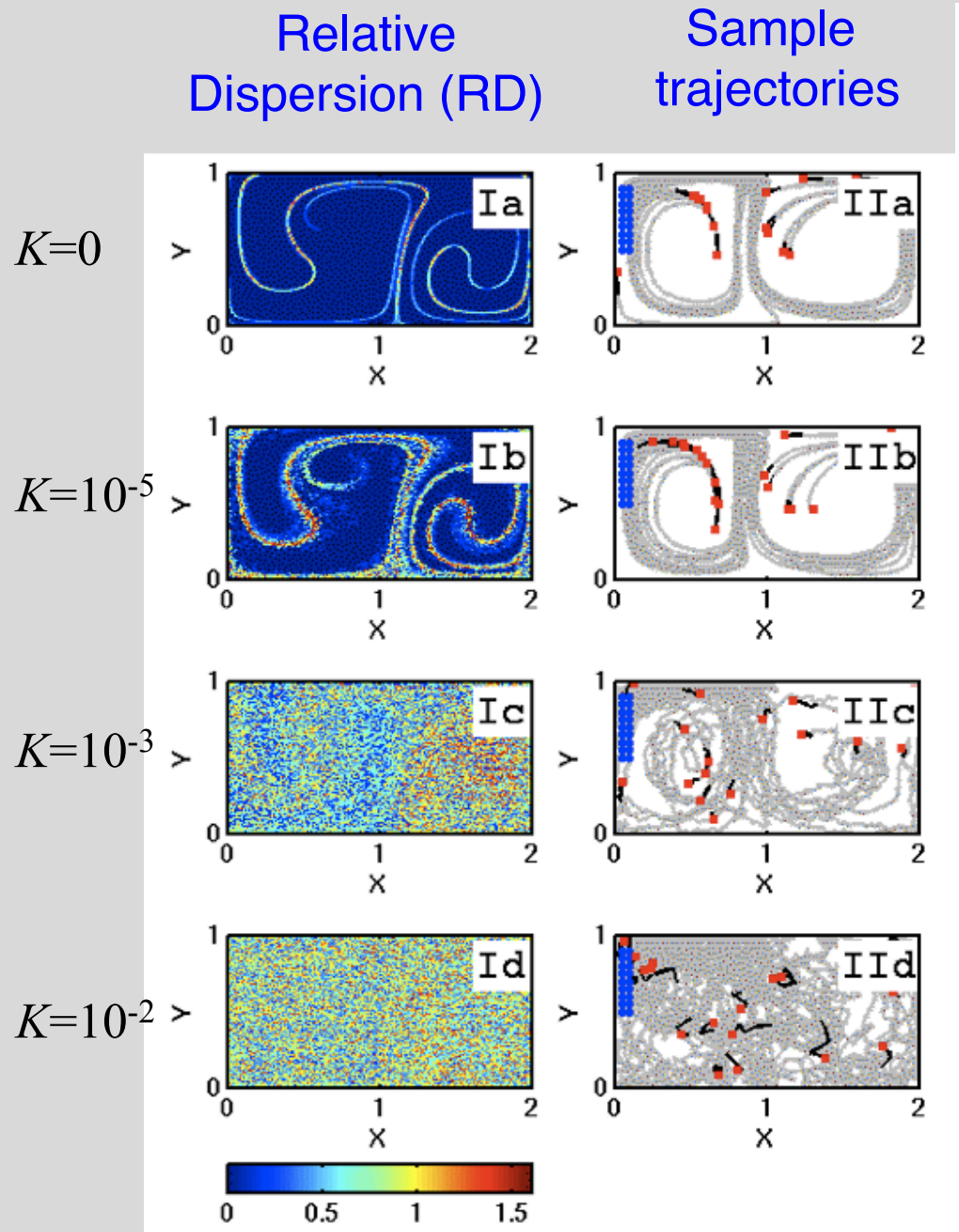

Time-dependent double gyre model

Relative Dispersion (RD)

Sample trajectories

PDF of RD

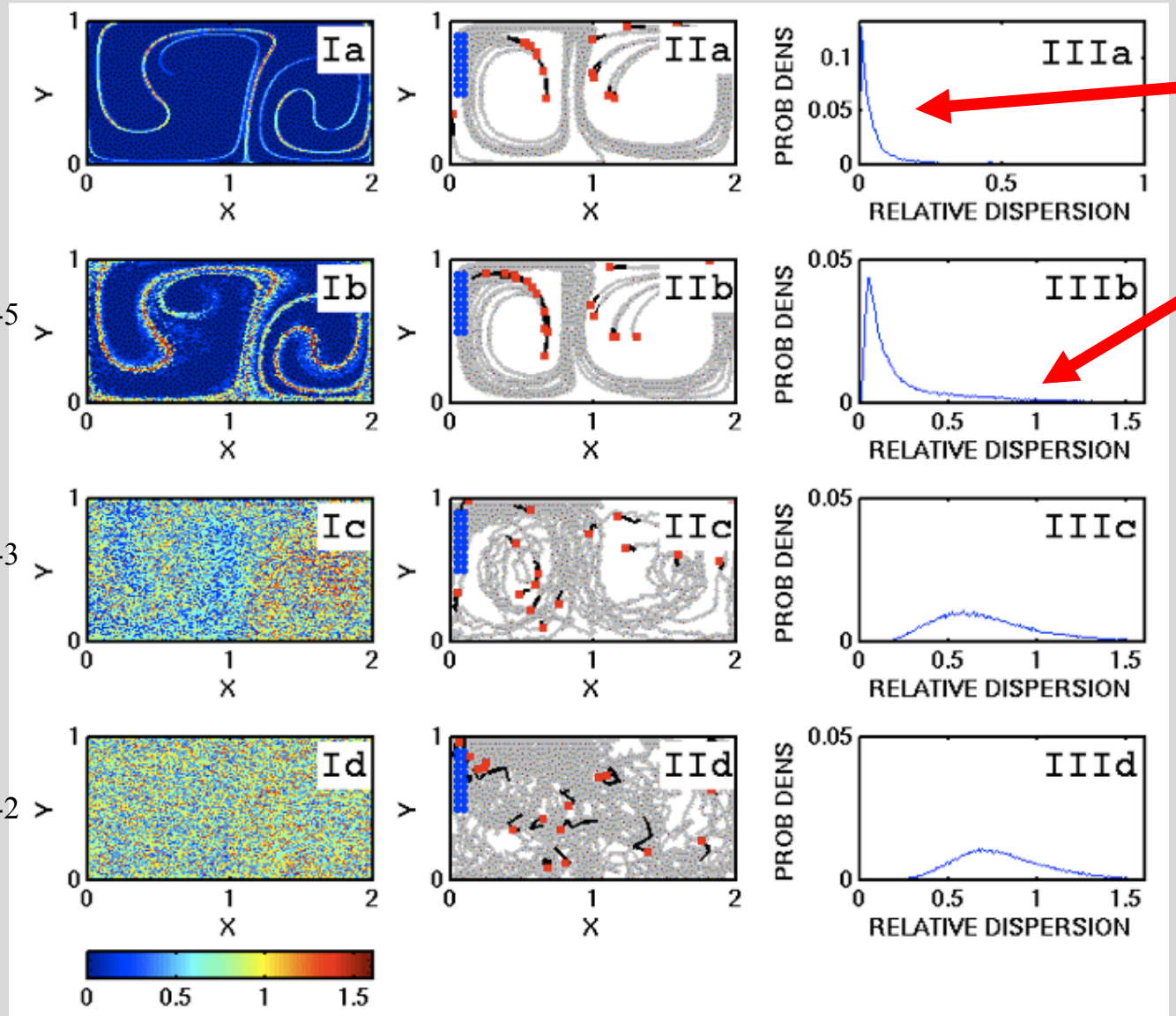

Large peak: “elliptic” trajectories with small RD.

Tail:“hyperbolic ” trajectories with high RD.

When K is increased, main peak shifts to the right. The influence on the barrier (tail), is manifested in the kurtosis

Time-dependent double gyre model

Kurtosis of RD as function of K

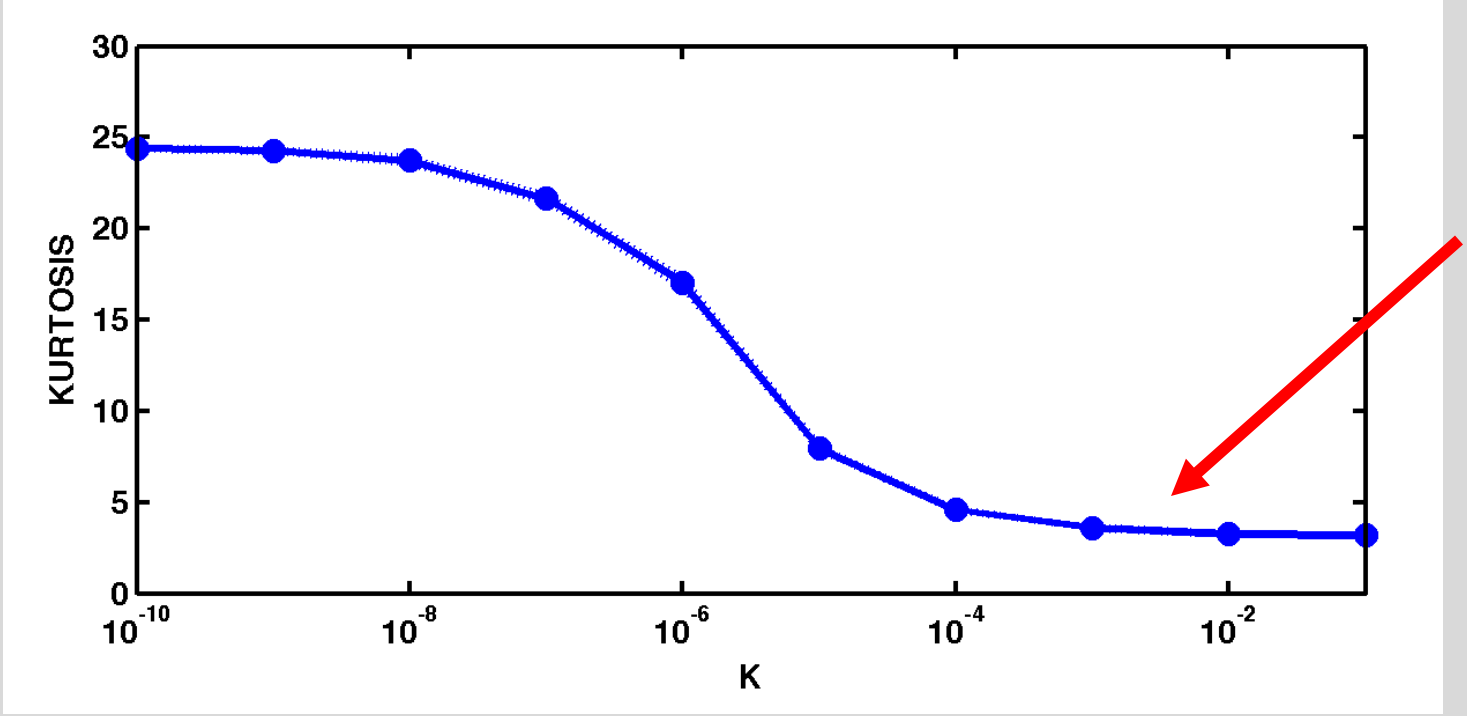

- At low *K*, kurtosis is large due to the presence of barriers (high RD).
- Upper bound is located between 10^{-3} and 10^{-2}, as based on visual inspection.
- Based on 20 realizations; very small standard deviation.
- Time-independent velocities yield an order of magnitude larger value (as expected, since we neglect chaotic mixing).

Geophysical application: The Gulf of Eilat

Aerial photographs and relative dispersion showing the existence of persisting barriers to mixing

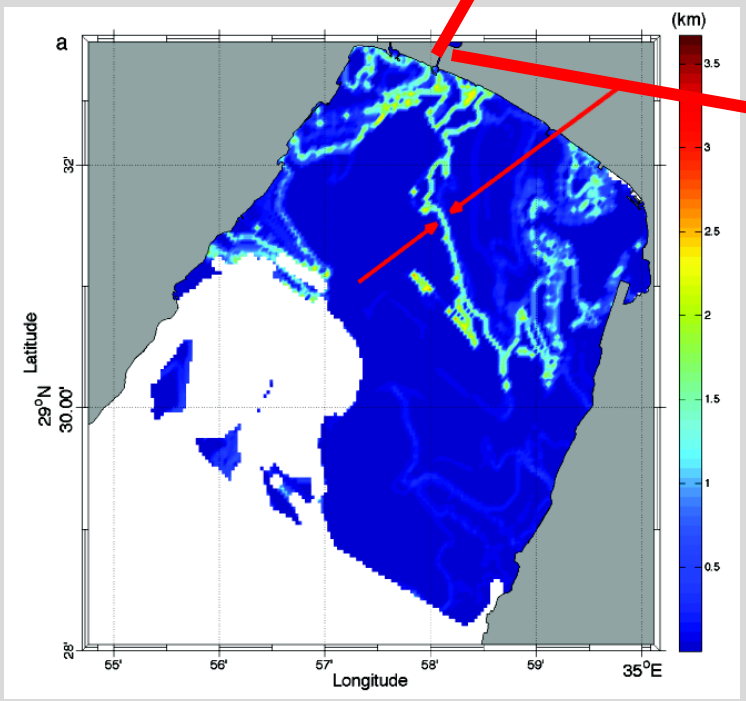

After two days

Geophysical application: The Gulf of Eilat

Relative Dispersion (RD) | Sample trajectories | PDF of RD

K=0

K=0.1

K=1

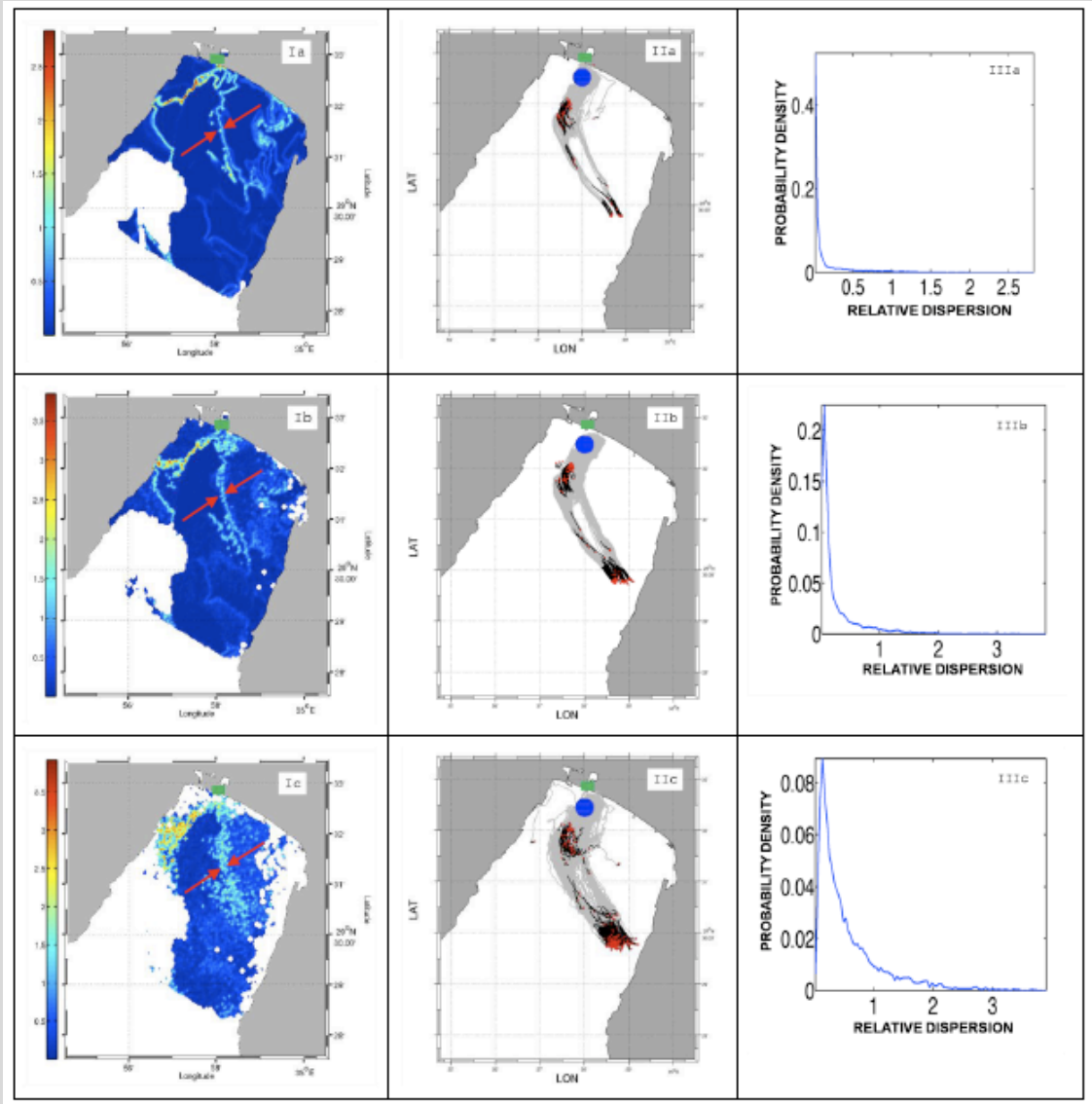

Geophysical application: The Gulf of Eilat

Kurtosis of RD as function of *K* for the Gulf of Eilat

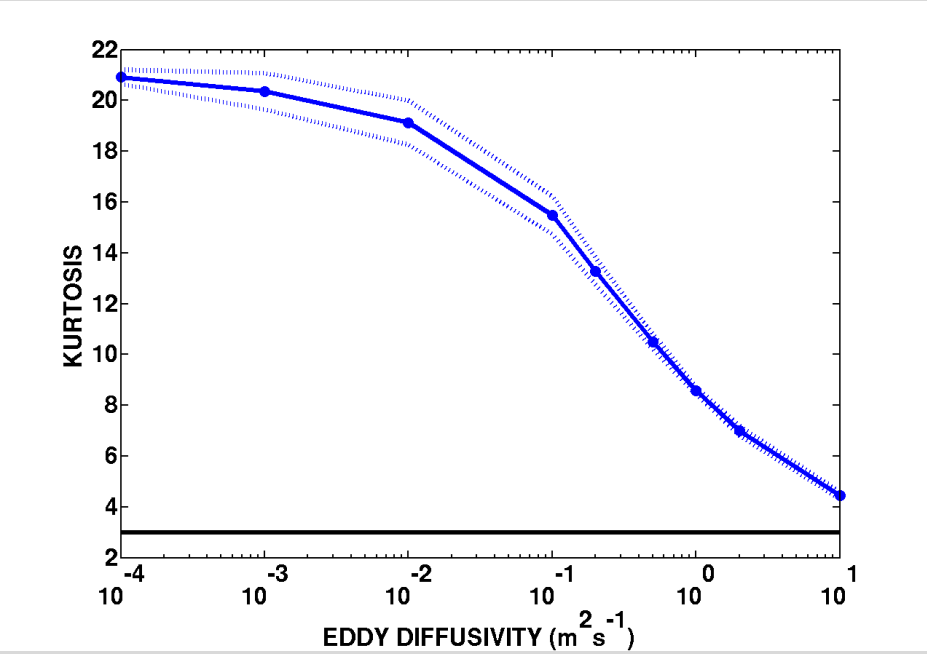

1. Scaling for the Gulf of Eilat: K=UL ~ 1-1000 m^2s^{-1}
2. The estimate of the upper bound based on visual examination of the relative dispersion is quantified by evaluating the response of the kurtosis of the RD as function of *K*.
3. Before the stochastic term is equal the deterministic term.

$$dX(t) = \mathbf{U}_{LS}\left(\mathbf{X}(t), t\right)dt + \sqrt{2K}\,dw(t)\,dt$$

Conclusions II:
Deducing an upper bound to the horizontal eddy diffusivity using a stochastic Lagrangian model

1. We propose a method to estimate an upper bound for *K* using a non-stationary zeroth-order stochastic Lagrangian equation by examining how mixing barriers present in a deterministic large-scale flow are eroded by adding eddy diffusivity.
2. The estimate of the upper bound based on visual examination of the relative dispersion is quantified by evaluating the response of the kurtosis of the RD as function of *K*.
3. Simple scaling arguments yield a wide range of possible values for the eddy diffusivity.
4. Before the stochastic term is equal the deterministic term.

$$dX(t) = \mathbf{U}_{LS}\left(\mathbf{X}(t), t\right)dt + \sqrt{2K}\,dw(t)\,dt$$

5. It is necessary to adequately resolve the "large scale" velocity field.

Carlson et al., *Environmental Fluid Mechanics*, 2010

When complexity leads to simplicity: Ocean surface mixing simplified by vertical convection

Rotem Aharon, Vered Rom-Kedar, and Hezi Gildor

Citation: Phys. Fluids **24**, 056603 (2012); doi: 10.1063/1.4719147

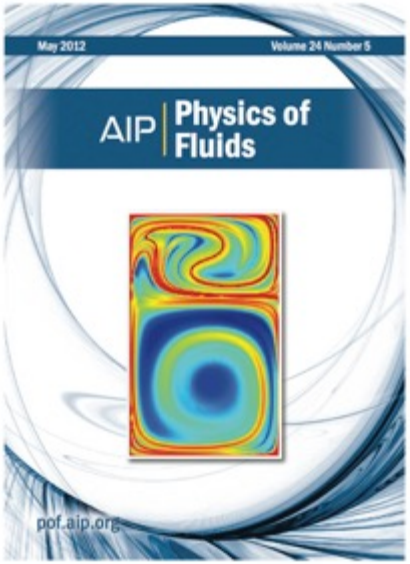

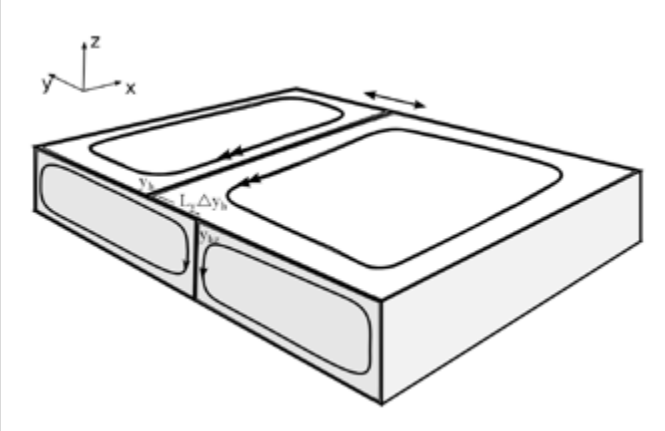

- Ocean motion is 3D; Naively, one would suspect that the small vertical component in geophysical flows will not play a significant role or will make mixing more complex.
- Counter intuitively, the very weak vertical motion often simplifies ocean surface mixing.
- This is demonstrated using the classical time-periodic double-gyre model. However, the results are general.

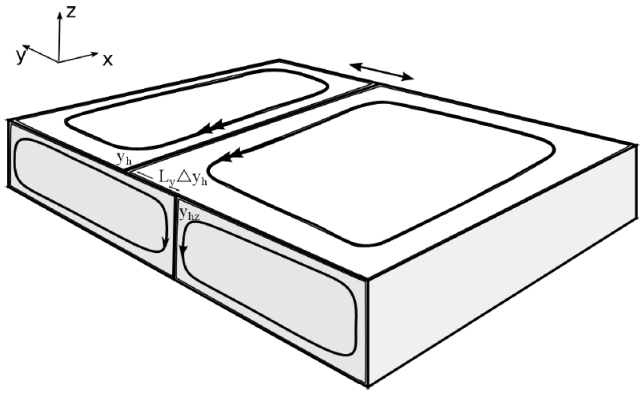

$$\mathbf{u}(x,y,t) = u_{double-gyre}\begin{pmatrix} u_{0x}(x,y) \\ u_{0y}(x,y) \end{pmatrix} + \epsilon u_{tide}\begin{pmatrix} u_{1x}(x,y,\omega_{tide}t+\theta_{tide};\epsilon) \\ u_{1y}(x,y,\omega_{tide}t+\theta_{tide};\epsilon) \end{pmatrix} + \epsilon u_{vert}\begin{pmatrix} u_{2x}(x,\omega_{day}t;\epsilon) \\ u_{2y}(y,\omega_{day}t;\epsilon) \end{pmatrix}$$

u_{tide}, u_{vert} – periodic functions

$u_{double\text{-}gyre}$, u_{tide} – area preserving

u is volume preserving

u_{tide}, u_{vert} may have similar order

$$\frac{U_{vert}}{U_{hor}}\frac{L_{hor}}{L_{vert}} \approx \frac{[0.001-0.01]m/s}{[0.1-0.3]\ m/s}\frac{10000m}{50-200m} \approx [0.1-20]$$

Usually different periodicities for the horizontal and vertical motions.

Underlying 3D flow is quasi-periodic in time, namely, deterministic and non-turbulent.

2D

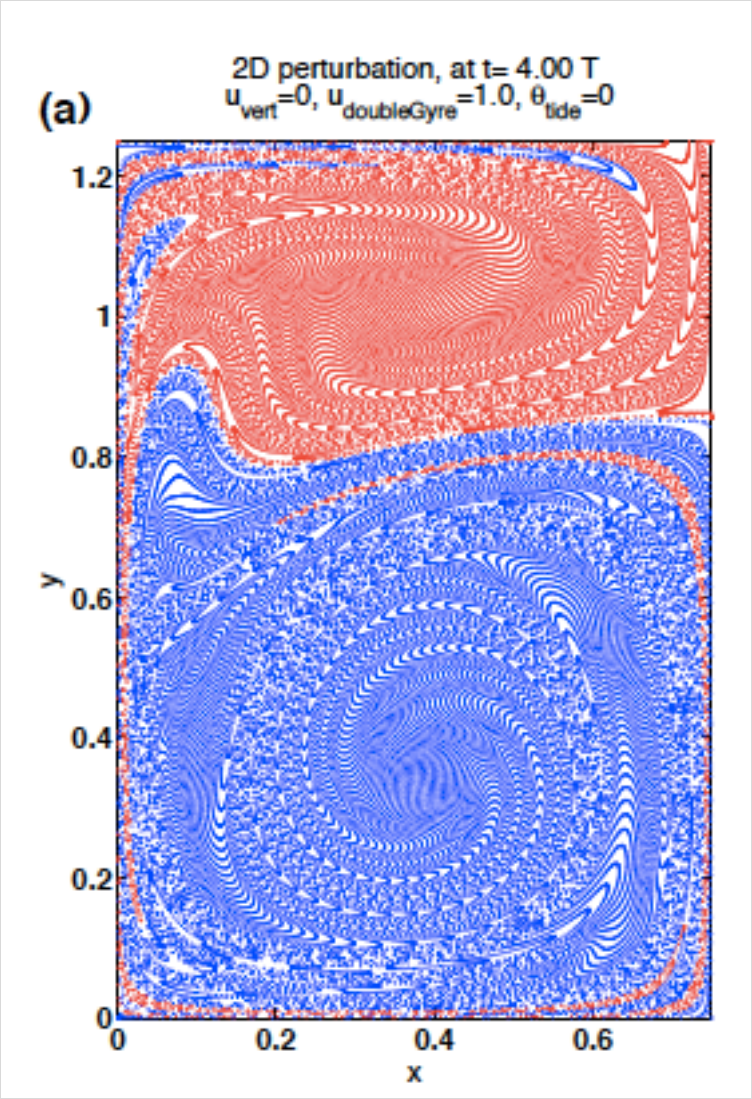

bidirectional flux

3D

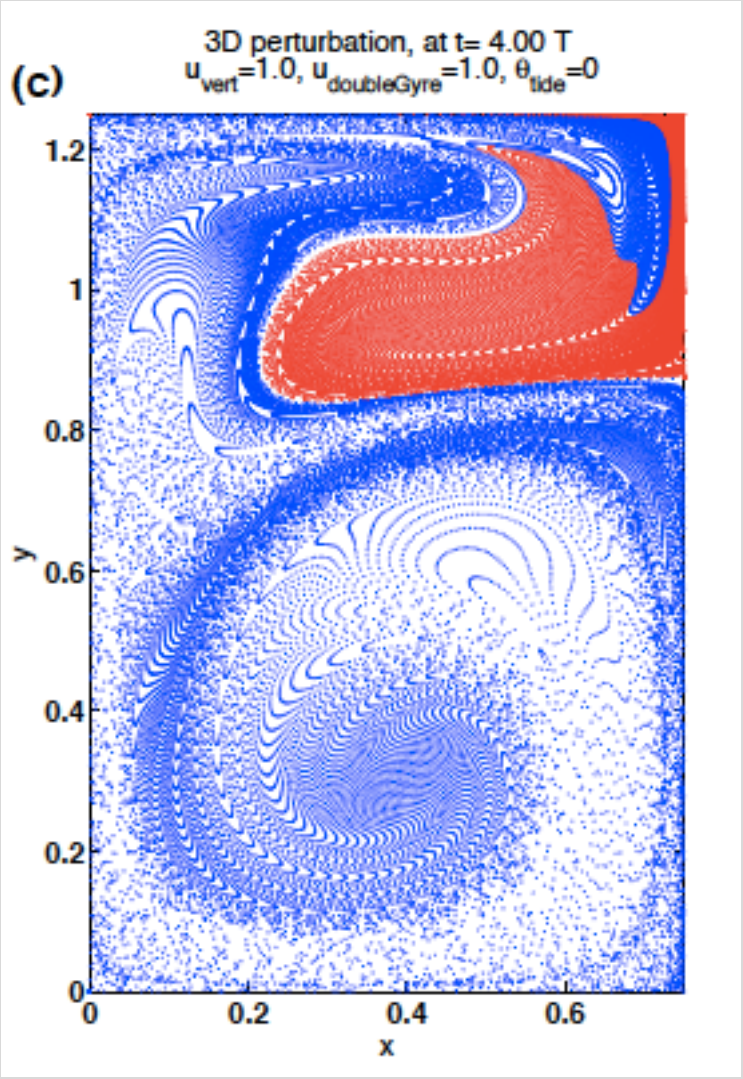

unidirectional flux

Sensitivity to the tidal phase and vigor of the horizontal flow

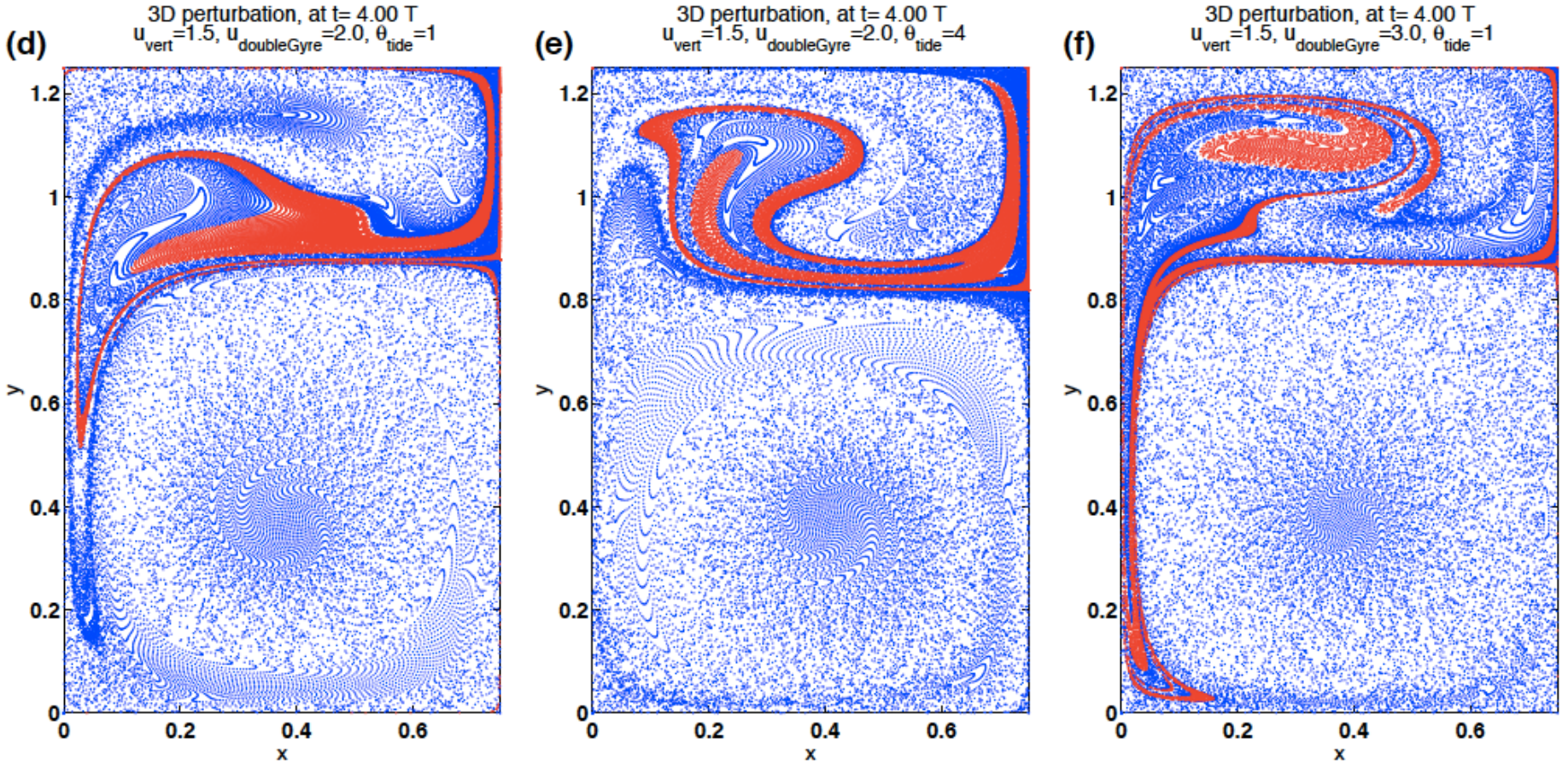

Why? Manifolds..: Theoretically, by Melnikov function:

* homoclinic tangles (bi-directional) * unidirectional flux

* phase dependent tangle

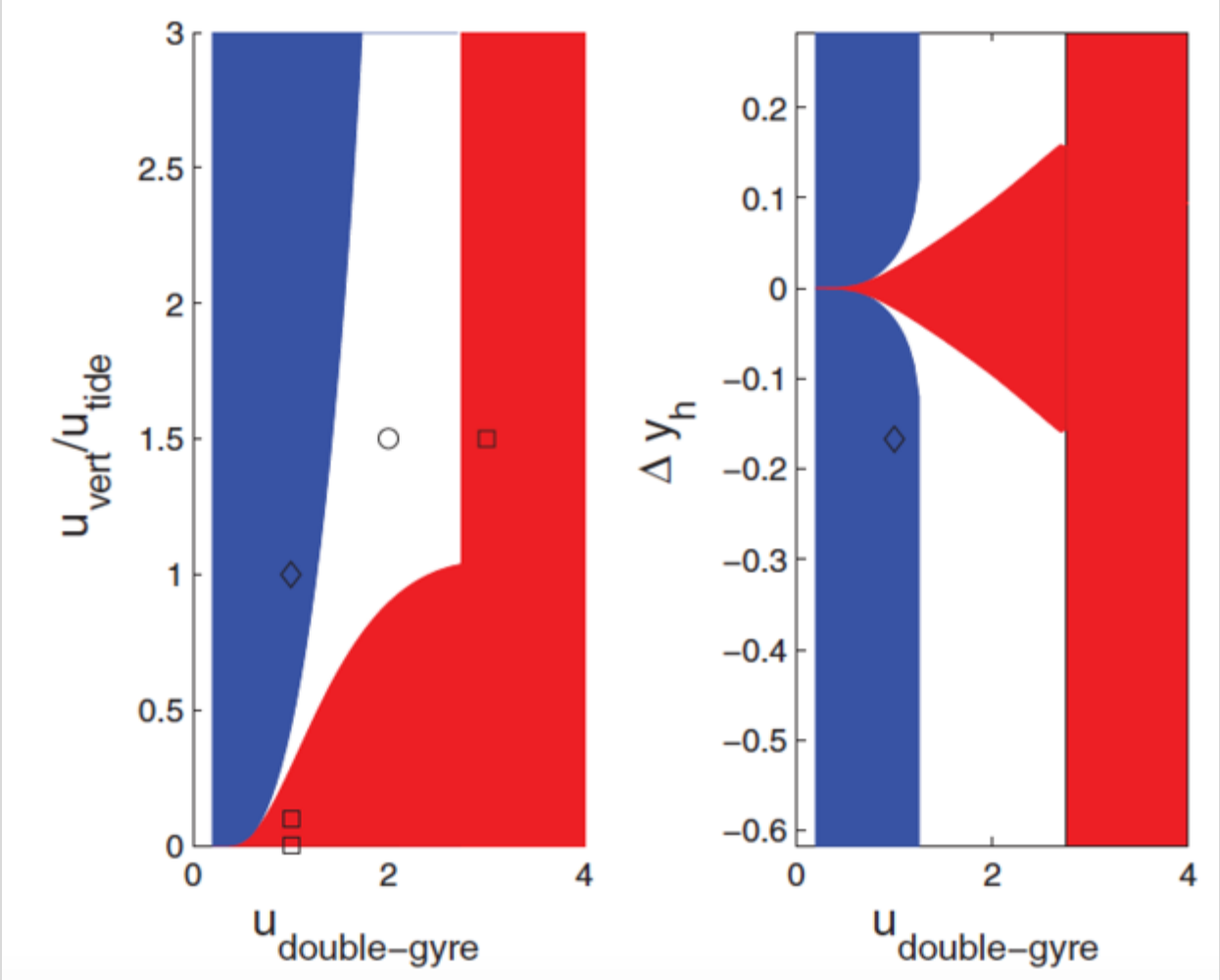

New Lagrangian diagnostics for characterizing fluid flow mixing

Ruty Mundel, Erick Fredj, Hezi Gildor, and Vered Rom-Kedar

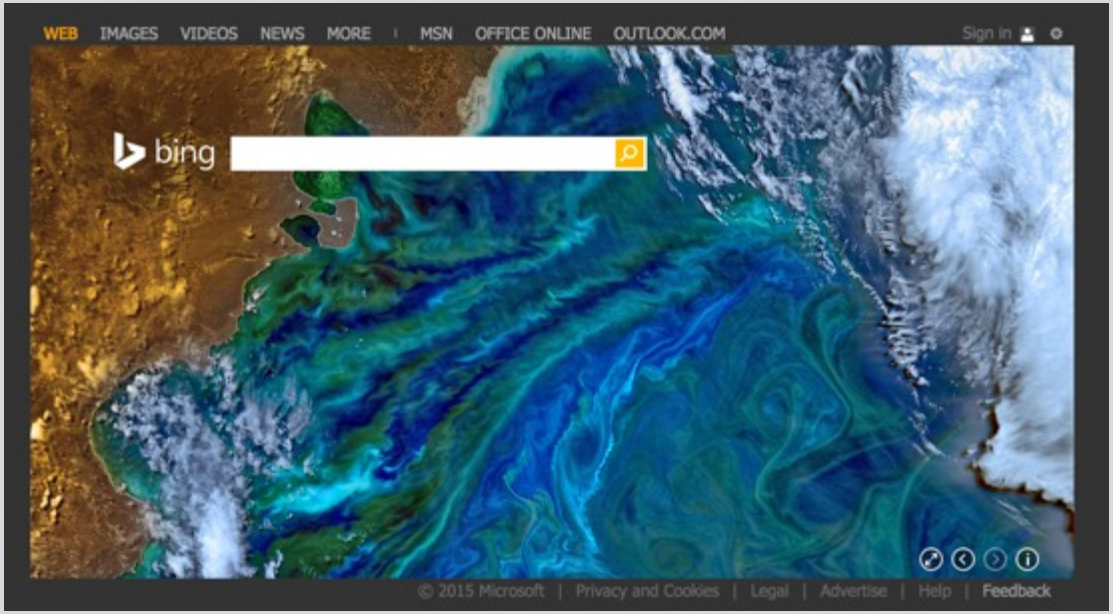

A phytoplankton bloom off the Atlantic coast of South America (© NASA)
World ocean day, June 8th

Extreme value fields

Flow: $$\frac{dx}{dt} = u(x,t), \qquad x \in \mathbb{R}^n,\ n = 2 \text{ or } 3$$

Extreme value fields, $[t_1, t_1 + \tau]$ is the extremal window:

$$\begin{aligned}
M_\phi^+(\tau; x_0, t_1) &= \max_{t \in [t_1, t_1+\tau]} \phi(x(t; t_0)), \\
M_\phi^-(\tau; x_0, t_1) &= \min_{t \in [t_1, t_1+\tau]} \phi(x(t; t_0)), \\
M_\phi^{shift}(\tau; x_0, t_1) &= M_\phi^+(\tau; x_0, t_1) - M_\phi^-(\tau; x_0, t_1), \\
M_\phi^{mean}(\tau; x_0, t_1) &= \frac{1}{2}(M_\phi^+(\tau; x_0, t_1) + M_\phi^-(\tau; x_0, t_1)),
\end{aligned}$$

f() : an observable

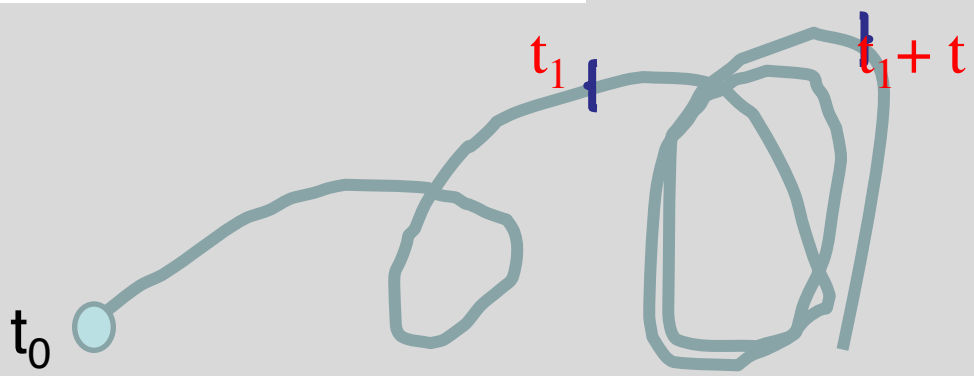

Extreme value fields

Examples of observables: maximal/minimal extent of trajectories (MET):

$$M_{\mathbf{r}}^{\pm}(\tau; x_0, t_1)$$

Future studies: Maximal velocities, maximal RD, maximal AD, maximal FTLE, maximal local stretching, etc,…

MET for the steady double gyre

- All i.c. in an ergodic component have the same MET value
- Typically, different ergodic components have different $M_r^{+,-}$
- CS have concentric MET field ➔ nearly linear PDF ➔ quadratic CDF
- The convergence is non-oscillatory in time

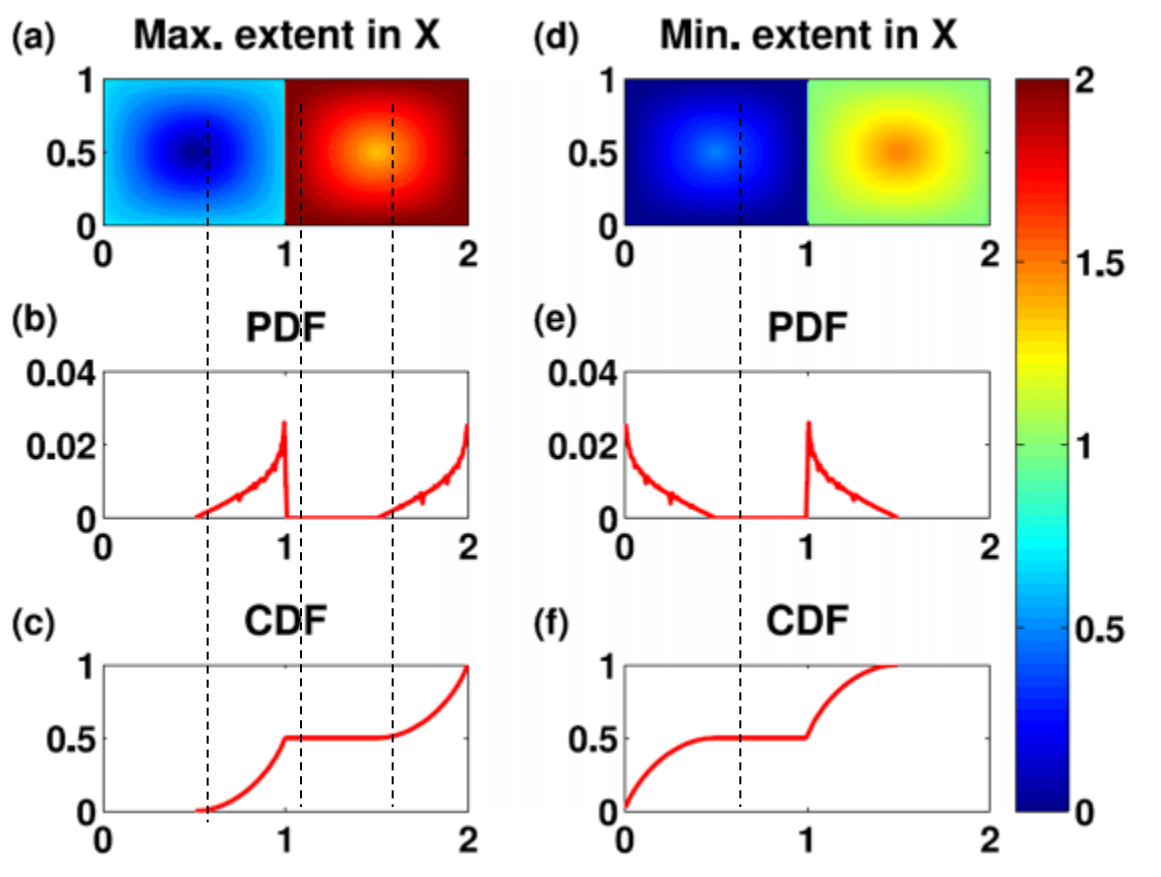

$$\Psi = -A \sin(\pi x)\sin(\pi y)$$

Resolving directions

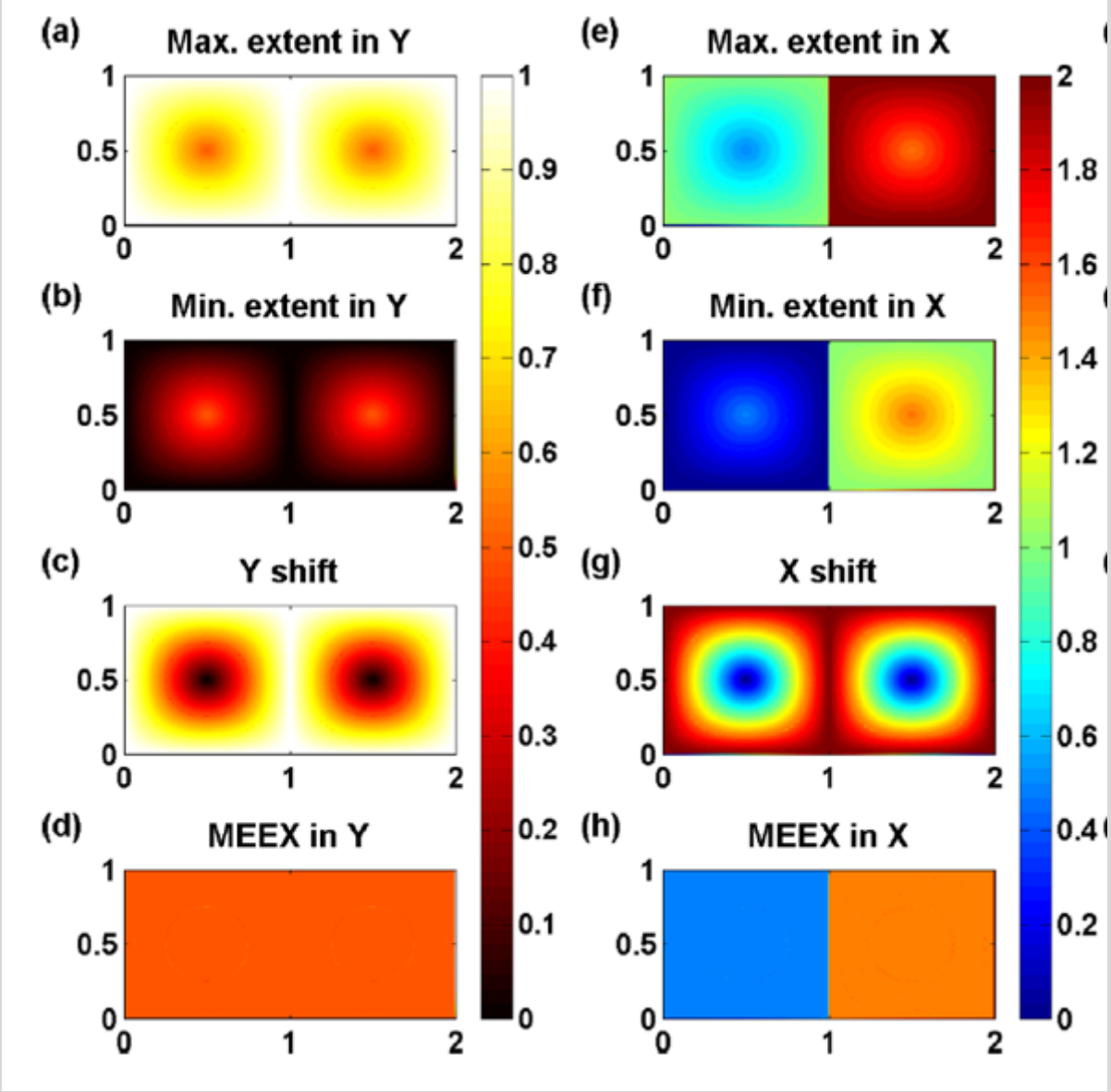

To use PDF and CDF need to choose a resolving ***r*** direction !

The information in the four different MET fields is not equivalent in the CDF representation!

MET for the unsteady double gyre

Mixing zone:

Discontinuous at the CS boundary – a nice detection tool!

A delta function in the PDF, a discontinuity in the CDF:

The CS are oscillating:

Center is still well defined

Oscillations are detectible by the mismatch from i.c.

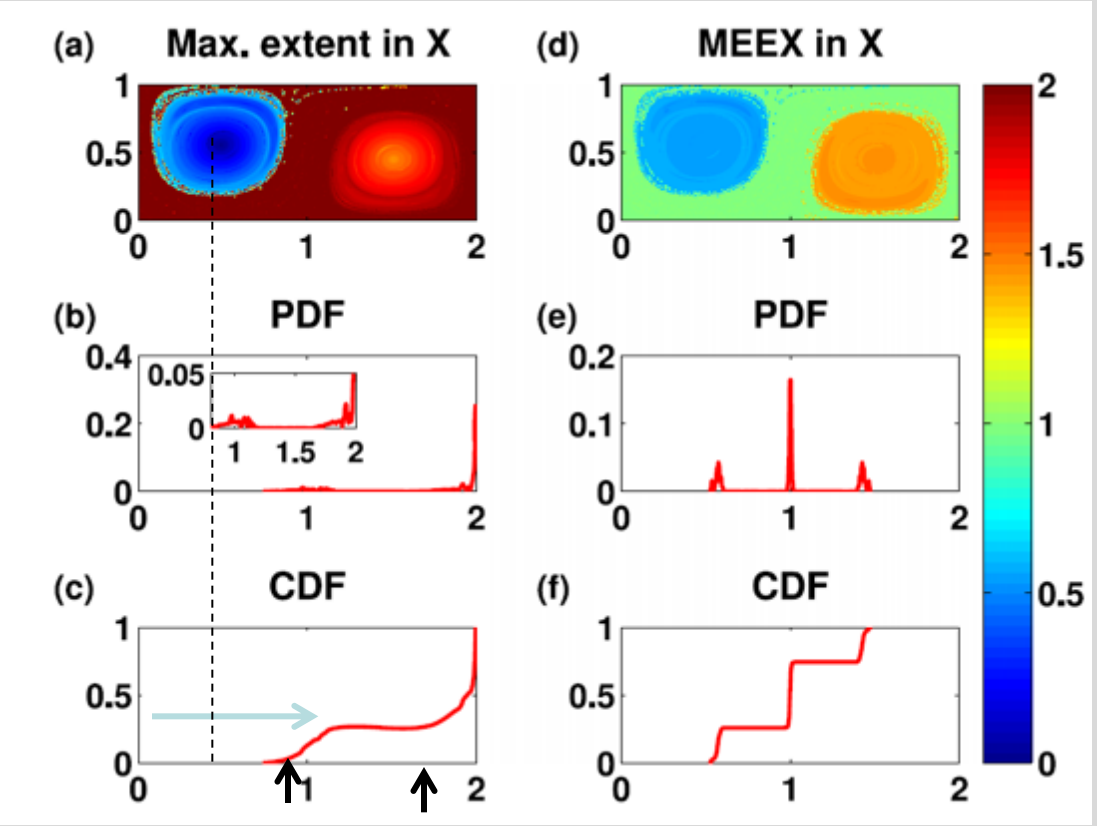

The CDF signatures of CS & mixing zones

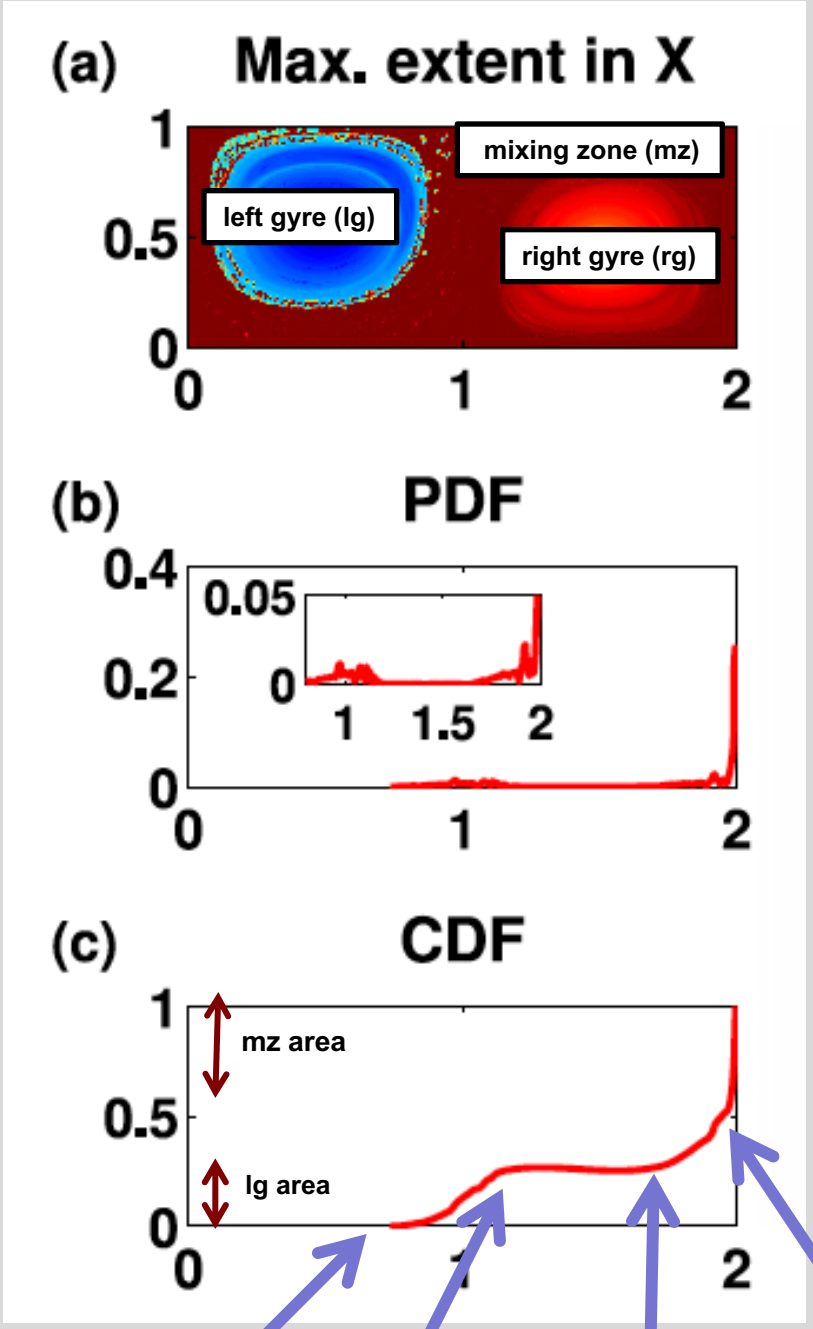

Sensitivity to flow intensity

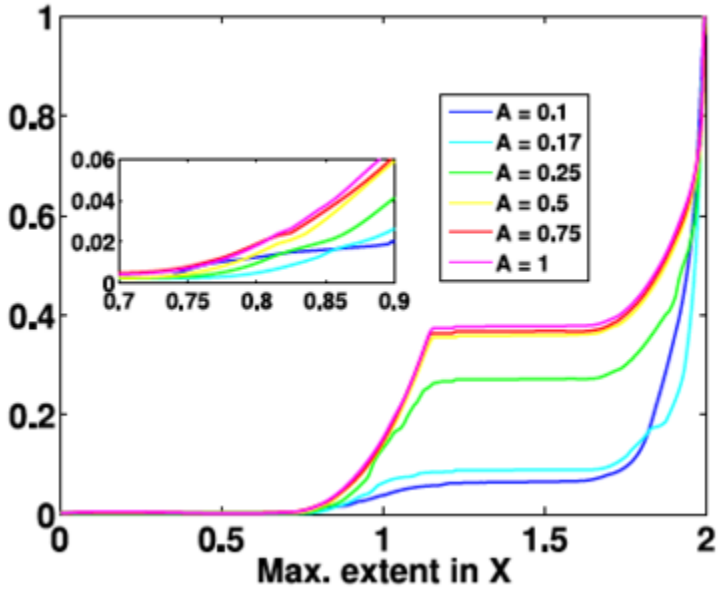

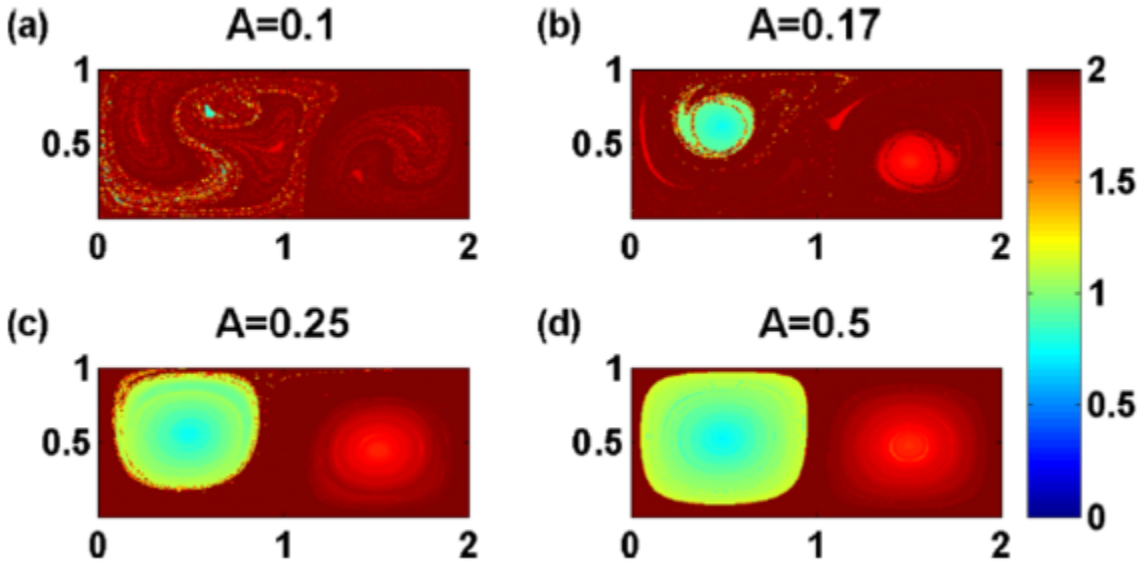

$$\Psi_{xy}(x, y, t) = -A \sin(\pi f(x,t)) \sin \pi y$$

$$f(x,t) = \epsilon \sin \omega t \; x^2 + (1 - 2\epsilon \sin \omega t)x.$$

$\epsilon = 0.25, \omega = 2\pi/10$ $t_1 = 0, \tau = 200$ (20 tidal periods)

Sensitivity to the number of periods

$$A = 0.17$$

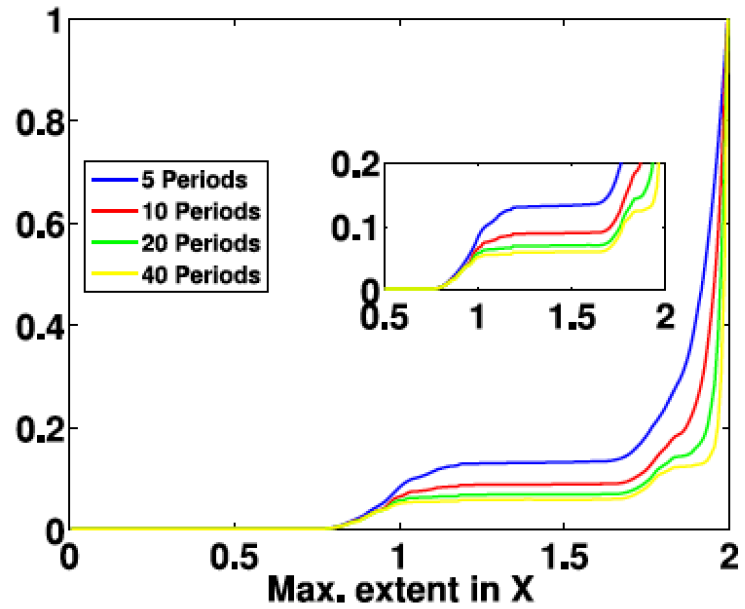

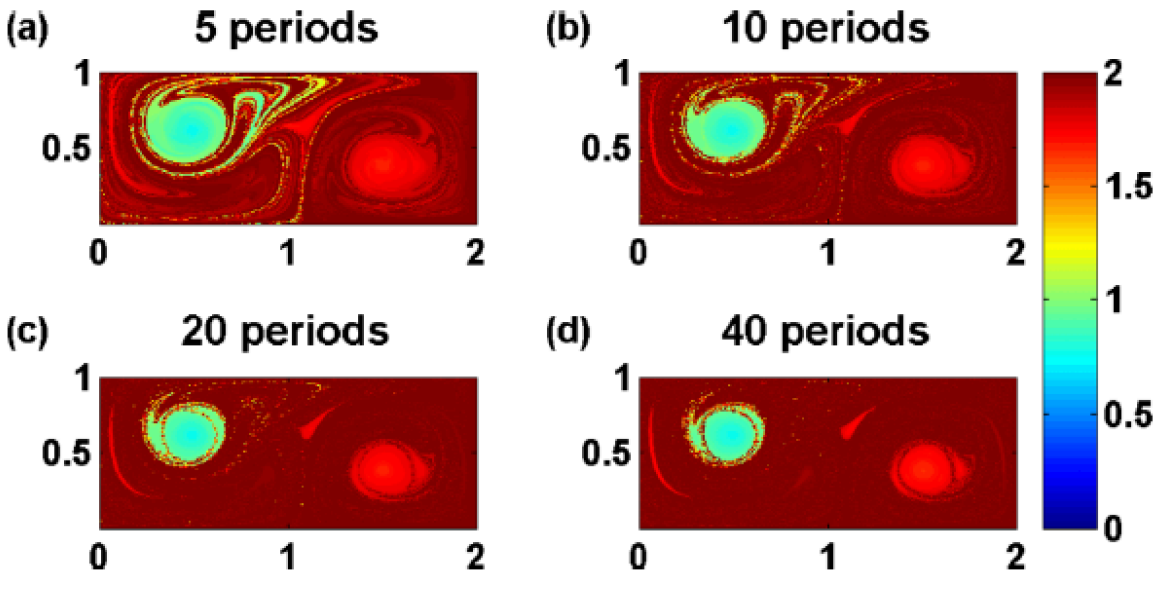

$$\Psi_{xy}(x, y, t) = -A \sin(\pi f(x,t)) \sin \pi y$$

$$f(x,t) = \epsilon \sin \omega t \; x^2 + (1 - 2\epsilon \sin \omega t)x.$$

$$\epsilon = 0.25, \omega = 2\pi/10$$

Dependence on spatial resolution

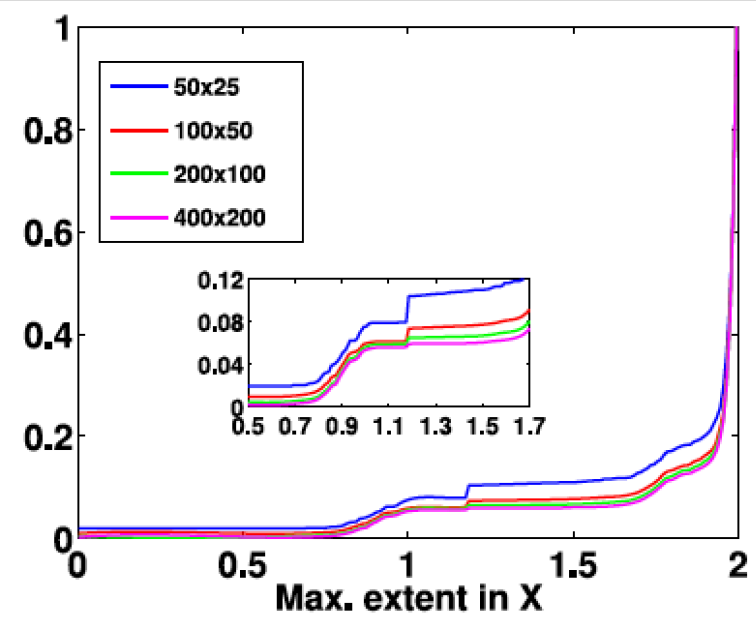

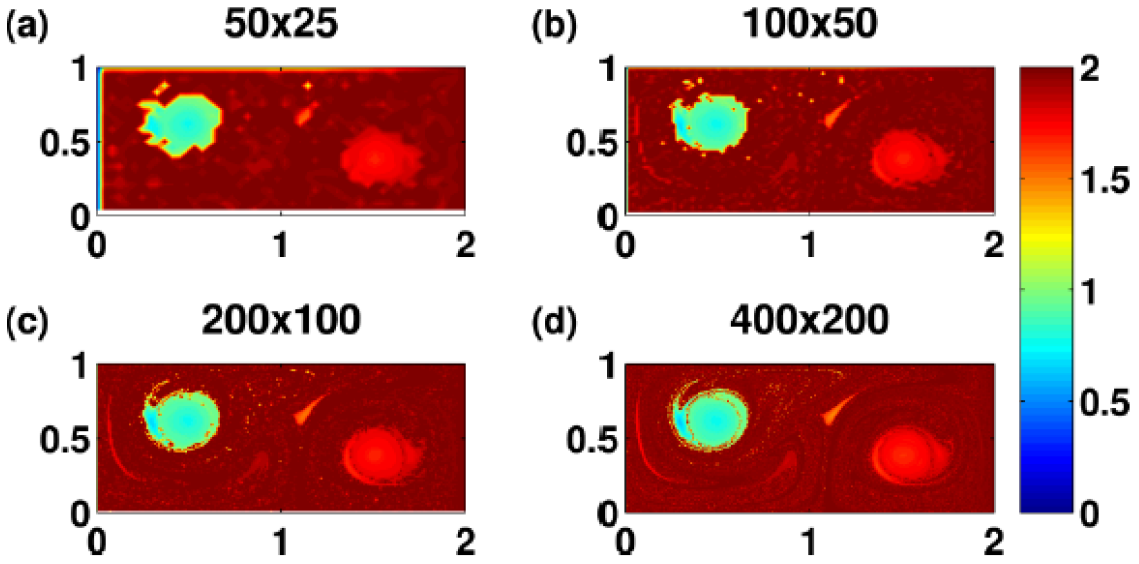

Relative dispersion:

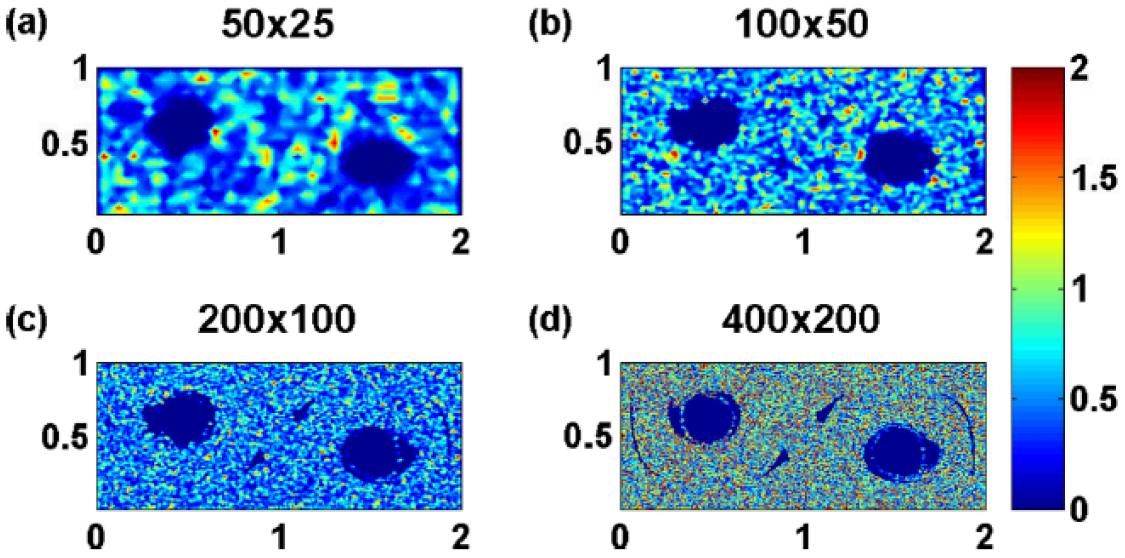

Geophysical application: South Atlantic

Okubo-Weiss field for November 22, 2006, based on AVISO data

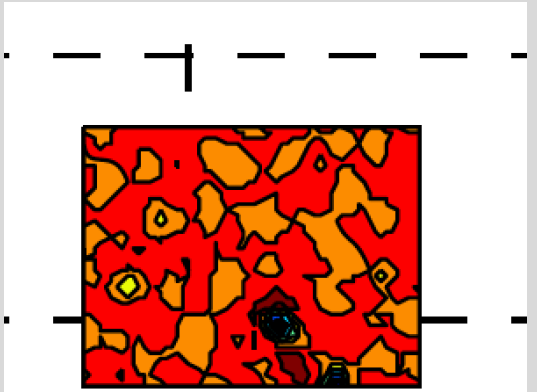

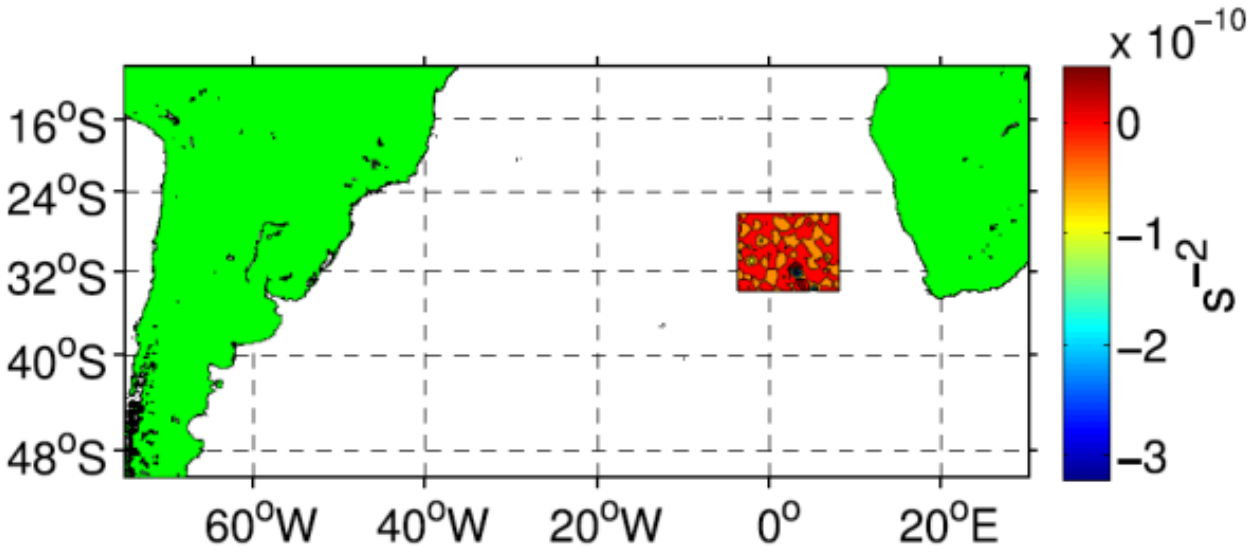

FIG. 13. The South Atlantic region in which particles are seeded on November 24, 2006 is the colored rectangular domain. The colors represent the Okubo-Weiss field (showing some spurious structures[57]) for November 22, 2006, the closest date to November 24, 2006 for which raw data from the AVISO data set are available.

Geophysical application: South Atlantic

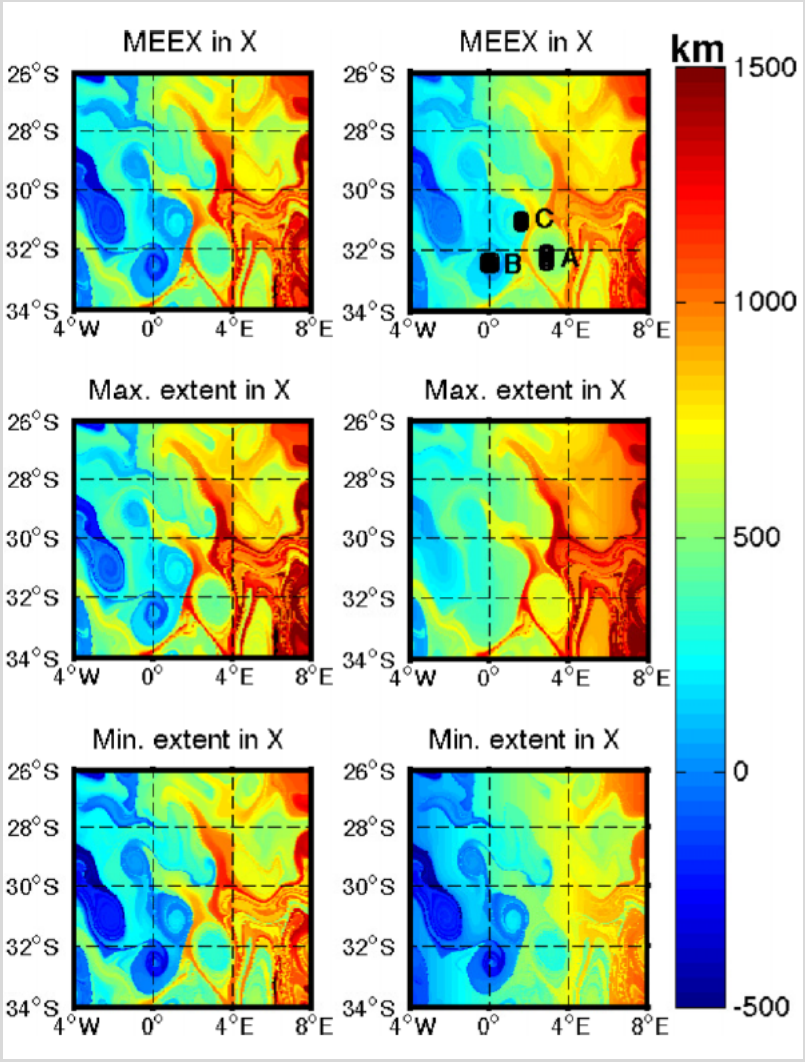

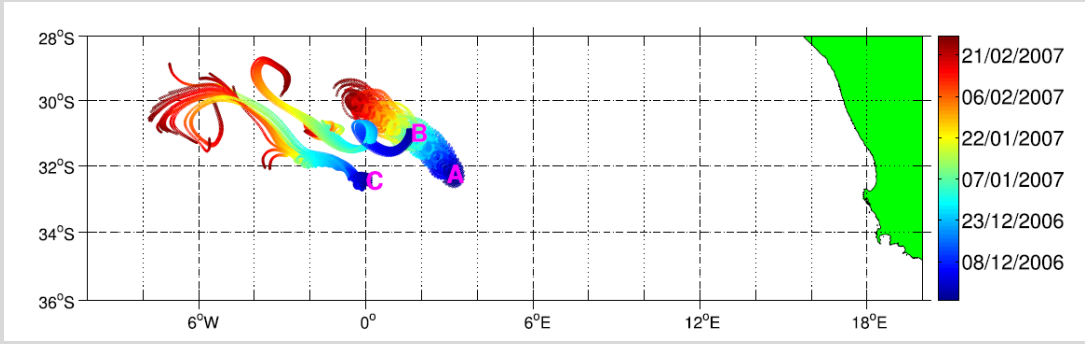

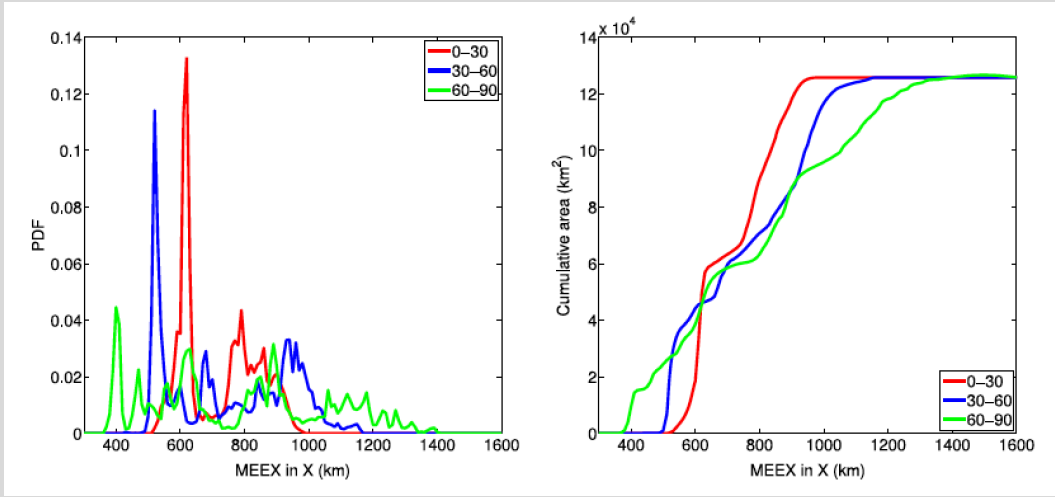

60-90 days

0-90 days

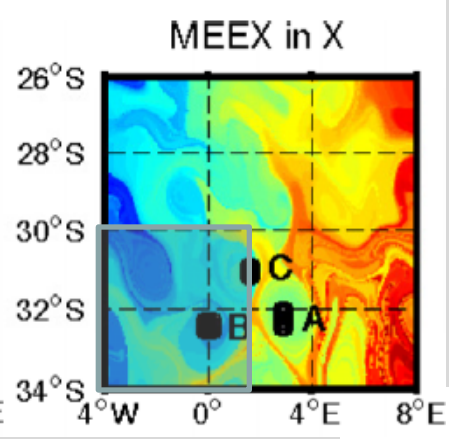

Identifying CS by subdivision of the domain

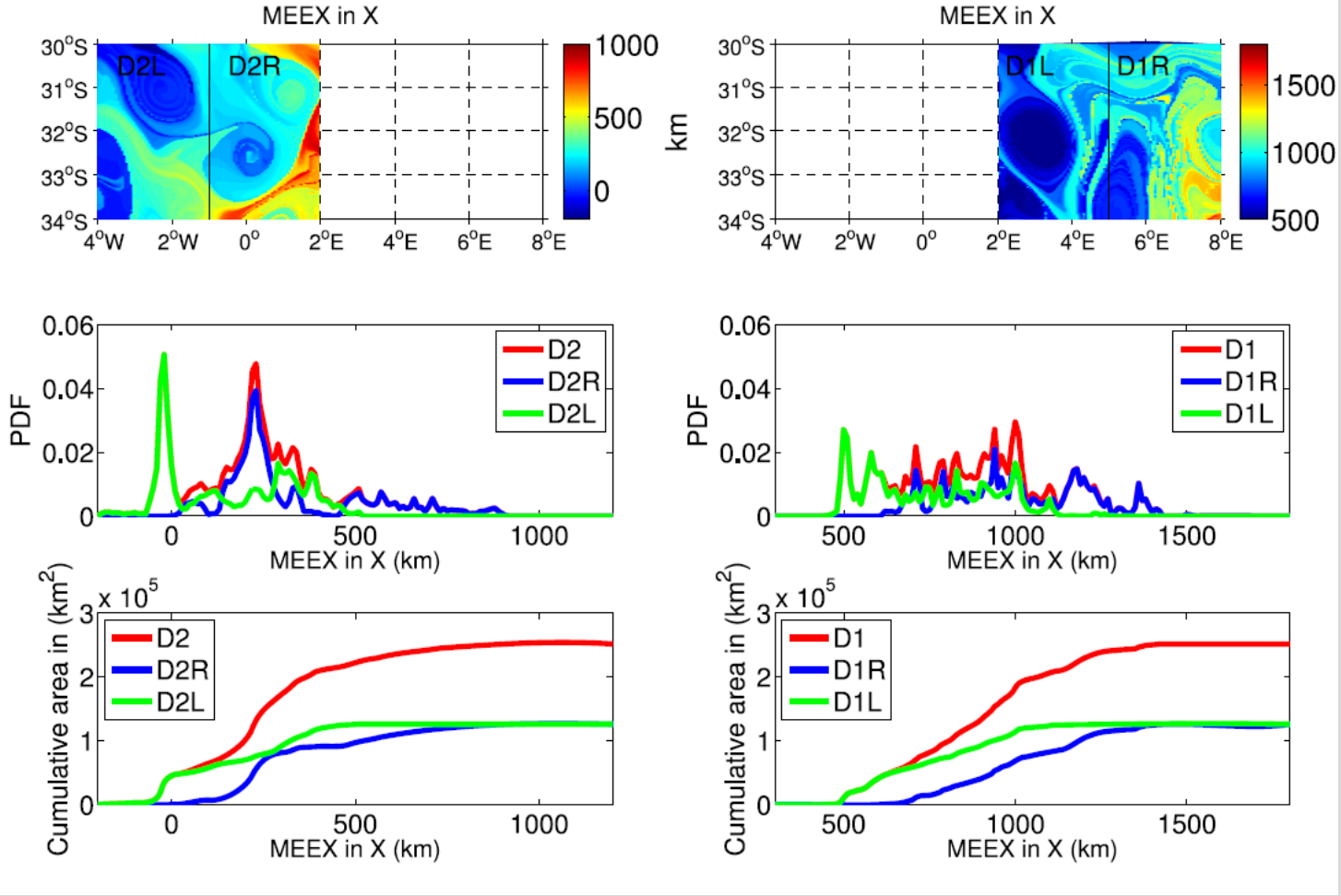

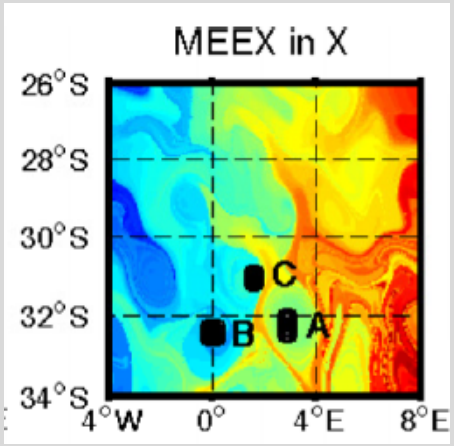

MEEX in Y

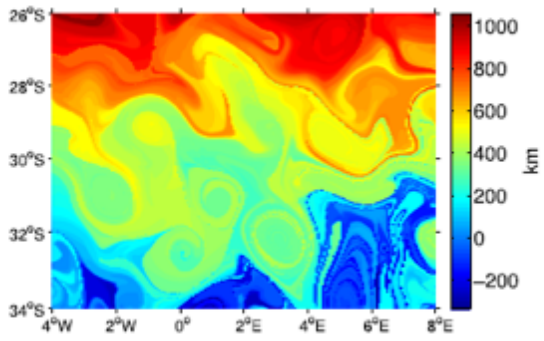

Relative Dispersion

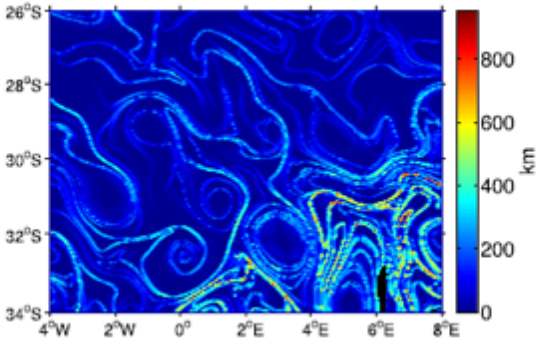

Absolute Dispersion

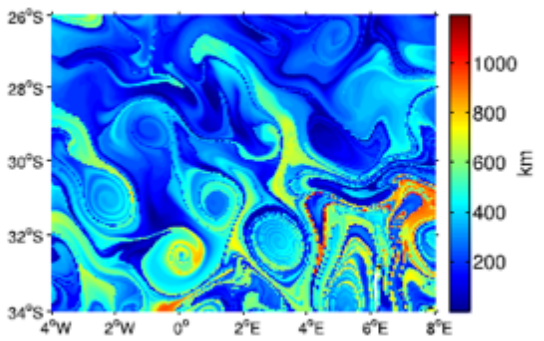

MET for open flows: CS signature in CDF

Open vortex pair

MEEX

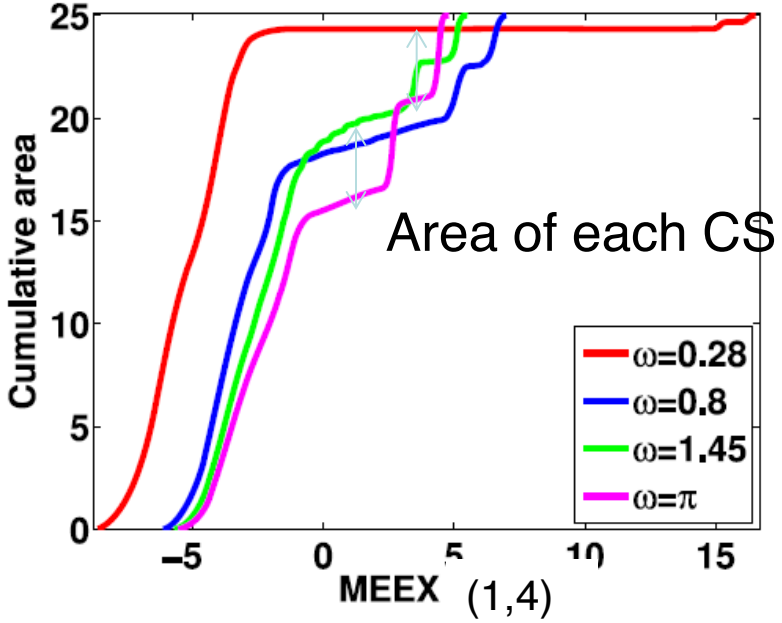

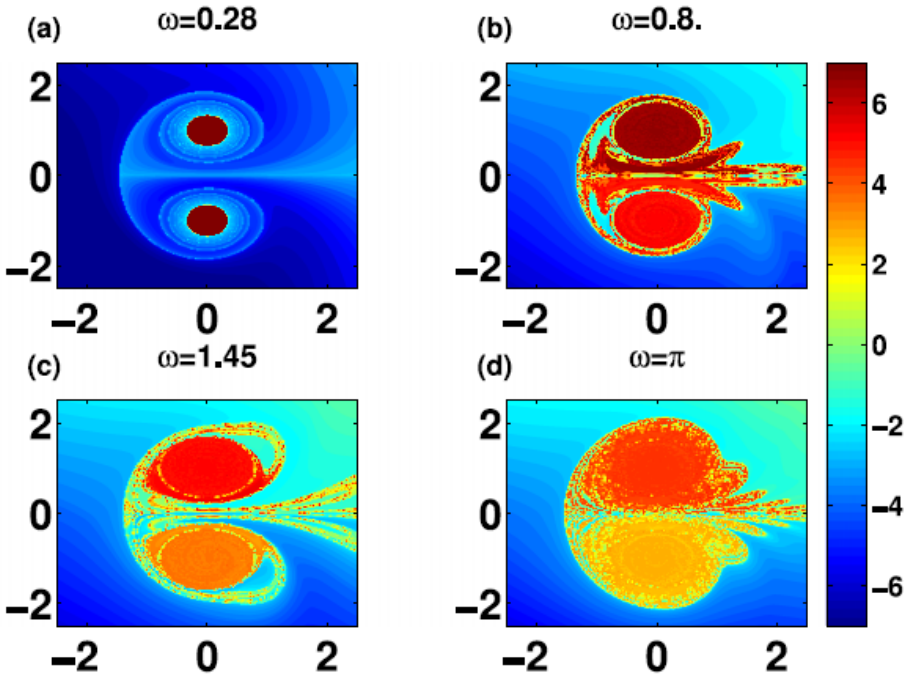

MET for open flows: time dependence

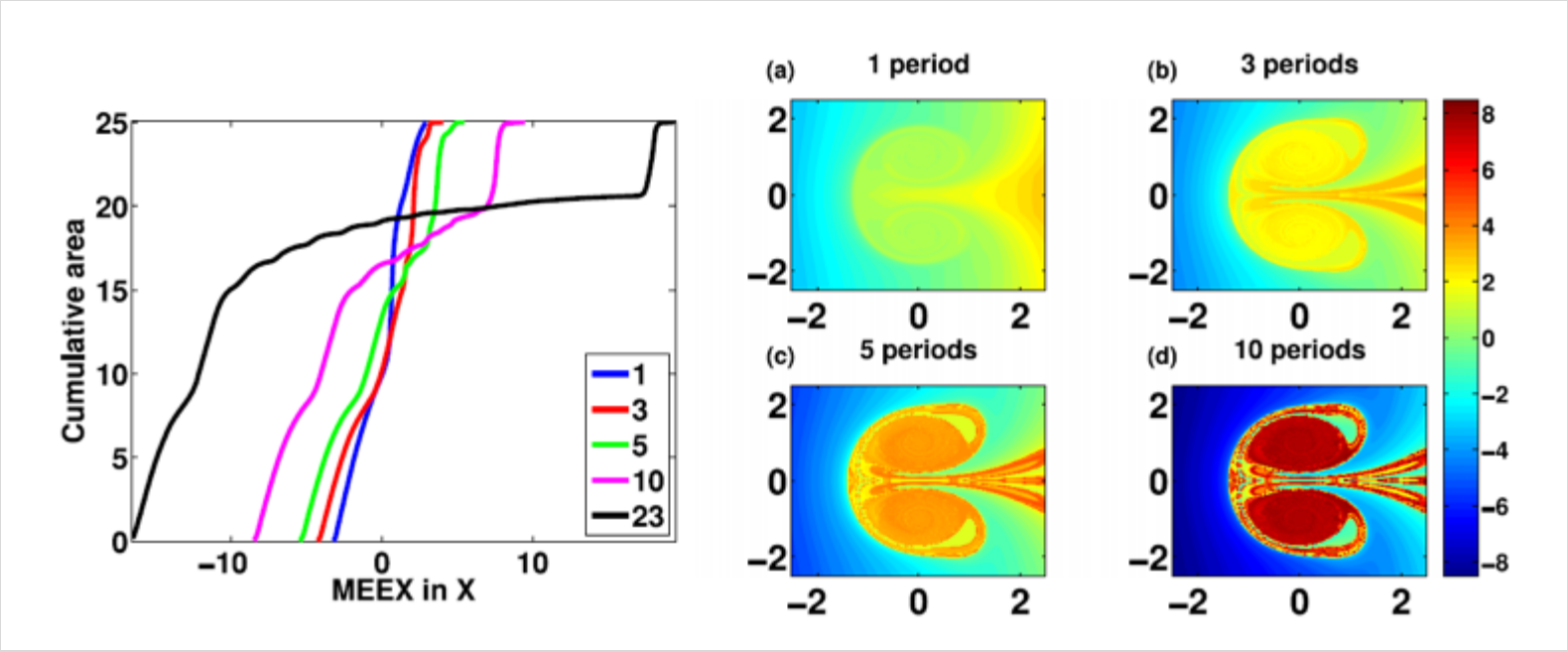

Vvortex = 0.5-Vfluid+O(ε)

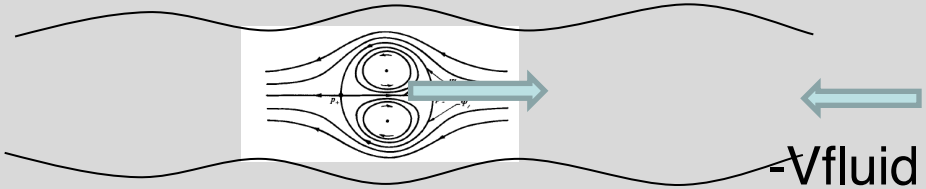

-Vfluid

Open flows: dependence on moving frame

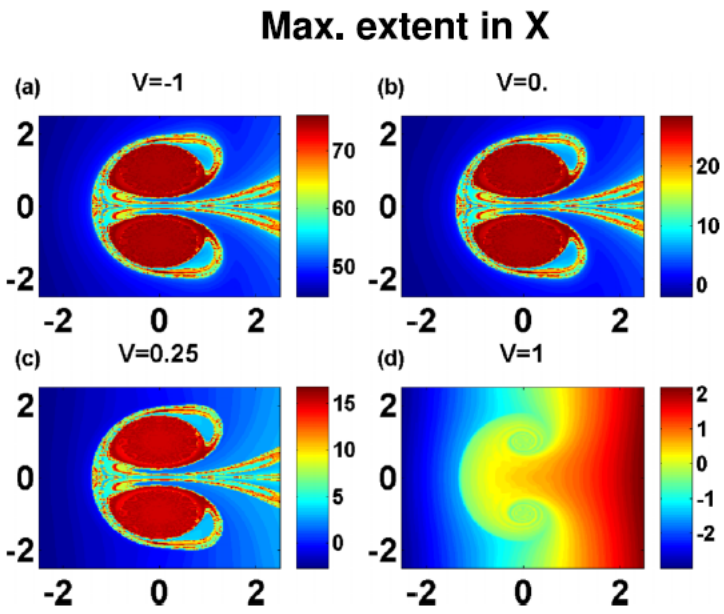

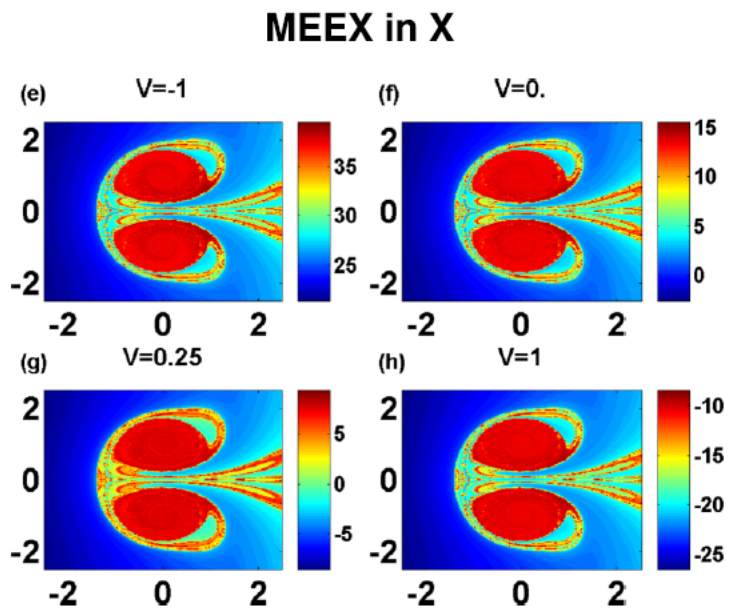

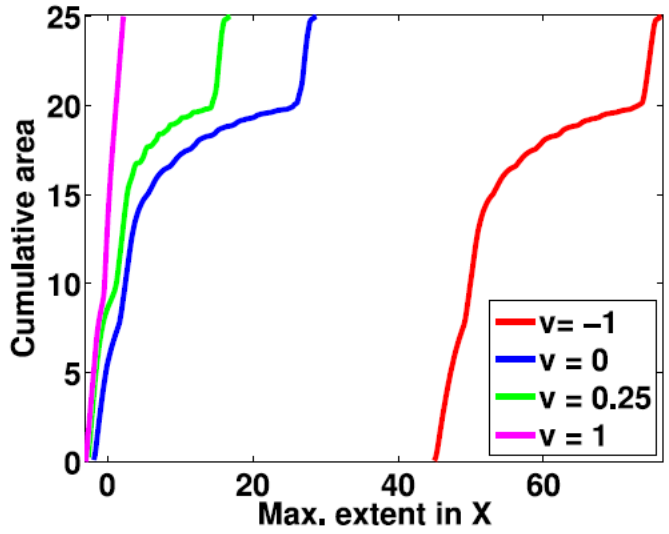

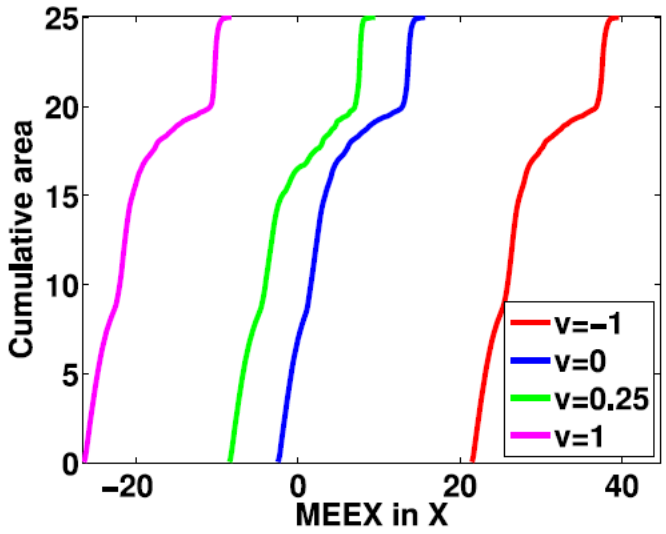

Open flows: dependence on extremal window

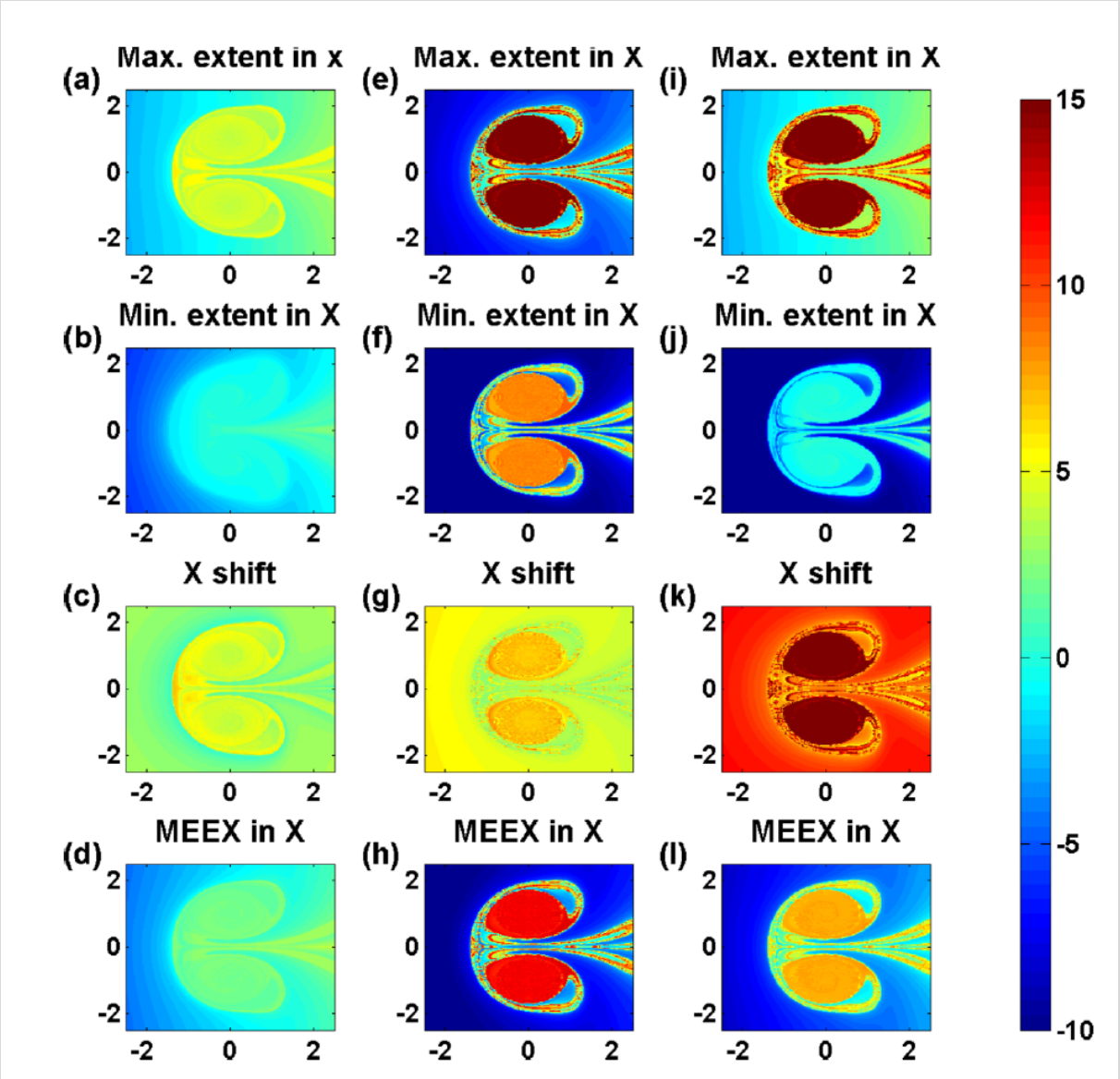

0-3 periods 7-10 periods 0-10 periods

- MET is a new simple diagnostic tools for identifying coherent structures in two- (and potentially three) dimensional unsteady flow
- ..and in both bounded and open domains.
- Simple and cheap computation; intuitive.
- Data reduction by using the PDF and CDF; sampling in few direction?
- Different asymptotic behavior than the RD/FTLE

Mundel et al., *Physics of fluids*, 26, 126602, 2014

Summary

- Differential advection in the ocean can lead to chaotic advection and to complex mixing of scalars.
- Lagrangian analysis is not trivial but provides important information for various applications.
- We demonstrate the existence of submesoscale barriers to mixing.
- In submesoscale geophysical flows, weak 3D flow associated with nocturnal convection typically simplifies the mixing.
- Combining visualization and velocity data (HF radar, altimetry) may help in identifying the effective eddy diffusivity.
- Still, relatively little work on 3D mixing.
- There are few user-friendly packages that simplify particle-tracking, with and without “behavior”.


Thank you!
"Always remember, a bad day at sea is better than a good day in the office",
Confucius.